TABLE IV. Calculation of $\Gamma(X \to 2\pi\gamma)$.

| | AI | AII | BI | BII |
|---|---|---|---|---|
| $R_X = \frac{\Gamma(X \to 2\pi\gamma)}{\Gamma(X \to 2\gamma)}$ | 13.5 or 45.0 | 13.3 or 6.1 | 13.5 or 54.3 | 13.3 or 5.0 |

and (54) lead to two values of $R_X$ for each solution given in Eqs. (22) and (23). These are tabulated in Table IV.

## VII. DISCUSSION

If, on the basis of the calculation for the ratio $\Gamma(\eta \to 2\gamma)/\Gamma(\pi^0 \to 2\gamma)$, we discard the lower value of the $\kappa$ mass used in solution B in Eqs. (23) and accept the solution AI over AII, we summarize the following results for the partial decay rates of the $X$ meson:

$$\begin{aligned} &\Gamma(X \to \eta\pi\pi) \simeq 6.0 \text{ MeV}, \\ &\Gamma(X \to 2\gamma) \simeq 95 \text{ keV}, \\ &\Gamma(X \to 2\pi\gamma) \simeq 1.3 \quad \text{or} \quad 4.3 \text{ MeV}, \end{aligned} \tag{57}$$

where we have quoted our results only for the MH quark model. We may remind ourselves that the value of $\Gamma(X \to \eta\pi\pi)$ is of course independent of the specific quark models. It is not possible to compare these results with the data, since the total width of $X$ is not yet accurately known.[22] If we take our results in Eqs. (57) seriously, then for the smaller of the two values for $\Gamma(X \to 2\pi\gamma)$ we have the ratio $\Gamma(X \to 2\pi\gamma)/\Gamma(X \to \eta\pi\pi) \simeq 0.2$, which is not far from the experimentally quoted[22] value of about 0.3 However, the width for $X \to 2\gamma$ seems to be too small.

A word of caution is necessary. Most of our calculations are based on the soft-$\eta$ approximation and we have no idea how good this approximation is. The fact that the Maki-Hara quark model seems to be preferred in our present calculations may also be spurious if, for instance, possible strong-interaction corrections to Eq. (38) do not drop out from the ratios of rates calculated in Sec. VI A, or if the mass of the $\kappa$ meson turns out to be much different from the value taken in obtaining the results (57).

[22] N. Barash-Schmidt *et al.*, Rev. Mod. Phys. **41**, 109 (1969). These tables quote an upper limit of 4 MeV for the decay width of $X$.

PHYSICAL REVIEW D VOLUME 1, NUMBER 7 1 APRIL 1970

# Unitary Padé Approximants in Strong-Interaction Physics: The Nucleon-Nucleon System

J. D. BESSIS, S. GRAFFI,* V. GRECCHI,* AND G. TURCHETTI†
*Service de Physique Théorique, Centre d'Etudes Nucléaires de Saclay, BP n° 2-91, Gif-sur-Yvette, France*
(Received 14 July 1969)

The unitary Padé approximants, successfully introduced in strong-interaction physics for the pion and kaon systems, are now applied to the nucleon-nucleon problem. It is assumed that the interaction between two nucleons is described by the renormalizable Lagrangian $L_I = ig\bar{\psi}\gamma_5\tau\psi\,\Phi + \lambda(\Phi\cdot\Phi)^2$. We present the result of the complete calculation of the [1,1] unitary Padé approximant, which does not involve the second term in the Lagrangian: This implies that no free parameters appear in our model. A complete description of low-energy nucleon-nucleon physics is then obtained which qualitatively and often quantitatively agrees with experiment. Bound states appear only in $S$ waves, and a real pole is found in the deuteron amplitude at 4.8 MeV when the pion-nucleon coupling constant is taken at its physical value $g^2/4\pi = 14.7$. The Regge trajectories rise with energy: The deuteron recurrence does not become physical, while the recurrences of the virtual $^1S_0$ state give rise to narrow resonances in the $^1D_2$ and $^1G_4$ waves. For all waves (with the exception of the $^1S_0$ which in the [1,1] Padé approximation has a wrong threshold behavior), the calculated phase shifts are in good qualitative agreement with the experimental phase-shift analysis.

## I. INTRODUCTION

IT is today a generally accepted belief that in strong-interaction physics one can only get, from the perturbative series, statements about the analyticity properties of the $S$ matrix. On the other hand, this standpoint does not allow us to infer quantitative information from the computation of the perturbative expansion. One may wonder whether it is the theory itself, or the most used approximation method, which is inadequate—i.e., whether the traditional perturbative approach, so successful in electrodynamics, is meaningless in the case of strong-interaction physics.

With this idea in mind, one has to look for other approximation schemes. Among the many possible techniques, one which seems to be particularly suitable is the Padé approximant method, which has been successfully introduced in strong-interaction physics for

* Istituto di Fisica, Università di Bologna.
† Istituto di Fisica, Università di Bari.

the $\pi$-$\pi$ and $\pi$-$K$ systems.[1,2] The purpose of the present paper is to apply this method to the oldest and perhaps the most classical problem of strong-interaction physics, the low-energy interaction between two nucleons.

This subject being classical, the literature on it is extremely large. Feshbach and Lomon[3] have reviewed the most recent developments from the standpoint of potential theory, and other reviews and books[4] may be consulted for general surveys, theoretical and experimental. Throughout this paper, we shall employ the relativistic formalism introduced by Goldberger, Grisaru, MacDowell, and Wong (hereafter GGMW),[5] and we shall assume, therefore, rigorous charge independence.

The choice of a renormalizable interaction Lagrangian will be based on the idea, generally accepted since Yukawa, that the pion is the most important generator of forces between two nucleons. Therefore, we shall neglect, in this approach, the existence of the other forces (such as $K\bar{K}$ forces, for instance). If one makes the standard invariance assumptions of quantum field theory together with isospin, parity, charge conjugation, and time-reversal invariance, then the most general renormalizable interaction Lagrangian involving only the nucleon and pion field one can write is

$$L_I = ig\bar{\psi}\gamma_5\boldsymbol{\tau}\psi\boldsymbol{\Phi}+\lambda(\boldsymbol{\Phi}\cdot\boldsymbol{\Phi})^2, \tag{1.1}$$

where $\psi$ is the nucleon and $\boldsymbol{\Phi}$ is the pion field, and $g$ and $\lambda$ are the pion-nucleon and pion-pion coupling constants, respectively.

The direct coupling between the pions, represented by the term $\lambda(\boldsymbol{\Phi}\cdot\boldsymbol{\Phi})^2$, not only is necessary in order to renormalize the theory (for nucleon-nucleon scattering, this necessity arises at eighth order in $g$), but also generates the pion-pion resonances, such as the $\rho$,[1] if one applies the Padé approximation method to the perturbative series in $\lambda$. Therefore, in this framework, possible effects due to vector mesons are automatically included in the theory, although they appear only in high-order perturbative terms. In the present paper, we compute only the first unitary Padé approximant to the two-body diagonalized $S$ matrix; as we shall see later, this approximant does not involve the term $\lambda(\boldsymbol{\Phi}\cdot\boldsymbol{\Phi})^2$ in the Lagrangian. In such a situation, our model has the very interesting feature that no free parameters appear; this is so because the pion-nucleon coupling constant $g$ is known to be about 14.

In such a case, and remembering that we are computing only the first Padé approximant, assuming isospin invariance, we think that it would be a satisfactory result to reproduce even qualitatively the actual low-energy nucleon-nucleon behavior. In fact, we shall see that better results are often obtained.

We wish to add some comments about the Lagrangian we have assumed. It is the simplest one which satisfies certain fundamental physical requirements. One can, of course, look for other Lagrangians satisfying further physical requirements [for instance, invariance under broken chiral symmetry and/or $SU(3)$ symmetry; PCAC, etc.]. In this first step, however, we restrict ourselves to the simple Yukawa Lagrangian, and this may be useful for two reasons: First, it is interesting to examine how our method works when it is applied to a theory whose possibilities in a purely perturbative formalism are well known. Second, it may constitute a good introduction to a more elaborate theory.

This paper is divided as follows. In Sec. II we give a general and brief review of the Padé approximation method, referring the reader frequently to other papers for a complete description. In Sec. III we apply the method to the relativistic formalism for nucleon-nucleon scattering as given in GGMW; in this context we discuss the threshold behavior of the partial-wave amplitudes, which is particularly important in a low-energy theory. In Sec. IV we treat the problem of the bound states of the two-nucleon system. Section V is devoted to a discussion of the deuteron. In Sec. VI the Regge trajectories of the deuteron and of the $^1S_0$ state are discussed. In Sec. VII we present the phase shifts predicted by our theory and compare them with the experimental ones and with those of the unitarized Born approximation. In Sec. VIII we present a general discussion of our results.

Appendix A is devoted to a sophisticated method for computing Froissart-Gribov integrals. Appendix B deals with notation, conventions, and technical details referring to nucleon-nucleon scattering. Appendix C deals with the explicit computation of the Feynman diagrams up to fourth order in $g$. Appendix D deals with a detailed discussion of the threshold behavior of the partial-wave amplitudes.

## II. PADÉ SOLUTION

### A. Generalities

We give in this section only a brief review of the Padé approximation method. The reader is referred to Wall[6] for the mathematical properties of the theory, and to Refs. 1 and 2 for its application to relativistic quantum

[1] D. Bessis and M. Pusterla, Nuovo Cimento **56**, 832 (1968).
[2] J. L. Basdevant, D. Bessis, and J. Zinn-Justin, Nuovo Cimento **60A**, 185 (1969).
[3] H. Feshbach and E. Lomon, Ann. Phys. (N. Y.) **17**, 236 (1968).
[4] L. Hulthén and M. Sugawara, in *Handbuch der Physik*, edited by S. Flügge (Springer, Berlin, 1957), Vol. 39; M. H. MacGregor, M. J. Moravcsik, and H. P. Stapp, Ann. Rev. Nucl. Sci. **10**, 291 (1960); R. Wilson, *Nucleon-Nucleon Scattering* (Interscience, New York, 1963); G. Breit and R. D. Haracz, in *High-Energy Physics*, edited by E. H. S. Burhop (Academic, New York, 1967), Vol. I; International Conference on the $N$-$N$ Interactions, Rev. Mod. Phys. **39**, 495–717 (1967).
[5] M. L. Goldberger, M. T. Grisaru, S. W. MacDowell, and D. Y. Wong, Phys. Rev. **120**, 2250 (1960). In this context see also M. L. Goldberger, Y. Nambu, and R. Oehme, Ann. Phys. (N. Y.) **2**, 226 (1957); D. Amati, E. Leader, and B. Vitale, Nuovo Cimento **17**, 68 (1960).
[6] H. S. Wall, *Continued Fractions* (Van Nostrand, Princeton, N. J., 1948).

field theory, and for further mathematical properties. Another exposition of the Padé method is given in Baker's paper.[7]

Given a renormalizable interaction Lagrangian, the renormalized perturbative expansion of the $S$ matrix in powers of the coupling constant can be computed:

$$S=I+gS_1+g^2S_2+\cdots+g^nS_n+\cdots. \quad (2.1)$$

Little is known about the convergence properties of this Taylor series around $g=0$, but it is generally believed that *the radius of convergence of this series is zero.* This is the case for many models, such as the one-dimensional relativistic models, the Peres model,[8] the four-dimensional $\lambda\Phi^3$ theory,[9] and the Bethe-Salpeter equation[10] or the Thirring model.[11] The same situation seems to hold even in electrodynamics, according to the arguments of Dyson[12] and of Frautschi[13]; in this case, however, the divergence of the perturbation expansion would have no *practical* importance: The series is then considered as an asymptotic series, because of the smallness of the coupling constant $\alpha=e^2/4\pi$; and, as is well known, very good numerical computations can be performed with such series.

In the case of the strong interaction, it appears that (2.1), as it stands, is useless. Because of the large value of the coupling constant, it does not behave at all like an asymptotic series. However, there exist powerful methods[14] by which, starting from a knowledge of the successive terms of the divergent Taylor expansion of a given function, one can reconstruct the function itself. Among many such methods, the method of Padé approximations appears to have remarkable mathematical properties and at the same time to be very efficient, when correctly applied to physical problems. The Padé method acts as an "accelerator of convergence" (in the case of divergent series, the acceleration is such that it transforms a divergent process into a convergent one).

We shall not repeat here all the detailed properties of such approximations, which can be found in the previous references, but we would like to summarize them.

### B. Properties of Padé Solution

From the Born series (2.1) cut off at order $2N$, one constructs a rational fraction in $g$, called the $[N,N]$ Padé approximation, which has the following properties.

(1) For small values of $g$, $[N,N](g)$ coincides with the Born series up to order $2N$.

(2) As a function of the *energy*, its analytical properties are the same as those of the Born series. This is important, because it is generally believed that the exact $S$ matrix has the same analytical properties in the energy as its *renormalized* perturbative terms.

(3) Moreover, it has been proved[1,15] that two-body unitarity (coupled channels) is identically fulfilled.

(4) Mass spectra and generalized mass spectra (Regge trajectories) come out very naturally in this approximation as zeros of the denominators of the fractions.

(5) Amazingly, it can be shown that the Padé approximants are identical to the approximations derived by Cini and Fubini[16] from the Lippmann-Schwinger variational principle (see Ref. 1).

(6) The method can handle formal series of noncommuting matrices, and has various other advantages: It satisfies identically the factorization of residues, Hermitian analyticity, and so on.

(7) Finally, the most interesting property is that, while the Taylor series can only represent functions analytic in a circle, our approximations can easily represent functions with very bad types of singularities: The poles and zeros by clustering can reconstruct cuts, or by coalescing can build up isolated essential singularities.

(8) Crossing symmetry is not identically fulfilled by our approximation, which has been based on the diagonalized (in the angular momentum) $S$ matrix. Nevertheless, there is some crossing symmetry built in, due to the fact that the perturbative series had it. In practice, however, crossing symmetry can be tested numerically.[2] Finally, if one assumes an interaction Lagrangian in which several coupling constants appear, one has to state on what footing these constants are to be treated in the perturbative expansion.[17]

In the present case, looking at the interaction Lagrangian (1.1) that we have assumed, one can see that the first order in $g$ corresponds only to a vertex, while the first order in $\lambda$ already corresponds to a four-point amplitude. Therefore, we shall treat the parameter $\lambda$ on the same footing as $g^2$. This implies, as already stated, that up to fourth order the perturbation expansion does not involve contributions coming from the term $\lambda(\Phi\cdot\Phi)^2$ in the Lagrangian.

## III. APPLICATION OF METHOD TO NUCLEON-NUCLEON SCATTERING

### A. General Features of Nucleon-Nucleon Scattering

The nucleon-nucleon amplitude can be written, following GGMW, as

[7] G. A. Baker, Jr., in *Advances in Theoretical Physics*, edited by K. A. Brueckner (Academic, New York, 1965).
[8] G. Baker and R. Chisholm, J. Math. Phys. **7**, 1900 (1966).
[9] V. Glaser and K. Hepp (private communication).
[10] C. A. Hurst, Phys. Rev. **85**, 920 (1952).
[11] W. Thirring, Ann. Phys. (N. Y.) **3**, 91 (1958).
[12] F. J. Dyson, Phys. Rev. **85**, 621 (1952).
[13] S. C. Frautschi, Progr. Theoret. Phys. (Kyoto) Suppl. **8**, 21 (1958).
[14] J. Hadamard, *Leçons sur la théorie des séries divergentes* (Gauthier-Villars, Paris, 1922).
[15] J. L. Gammel and F. A. MacDonald, Phys. Rev. **142**, 1245 (1966).
[16] M. Cini and S. Fubini, Nuovo Cimento **11**, 142 (1954).
[17] S. Mignaco, M. Pusterla, and E. Remiddi, Saclay Report, 1969 (unpublished).

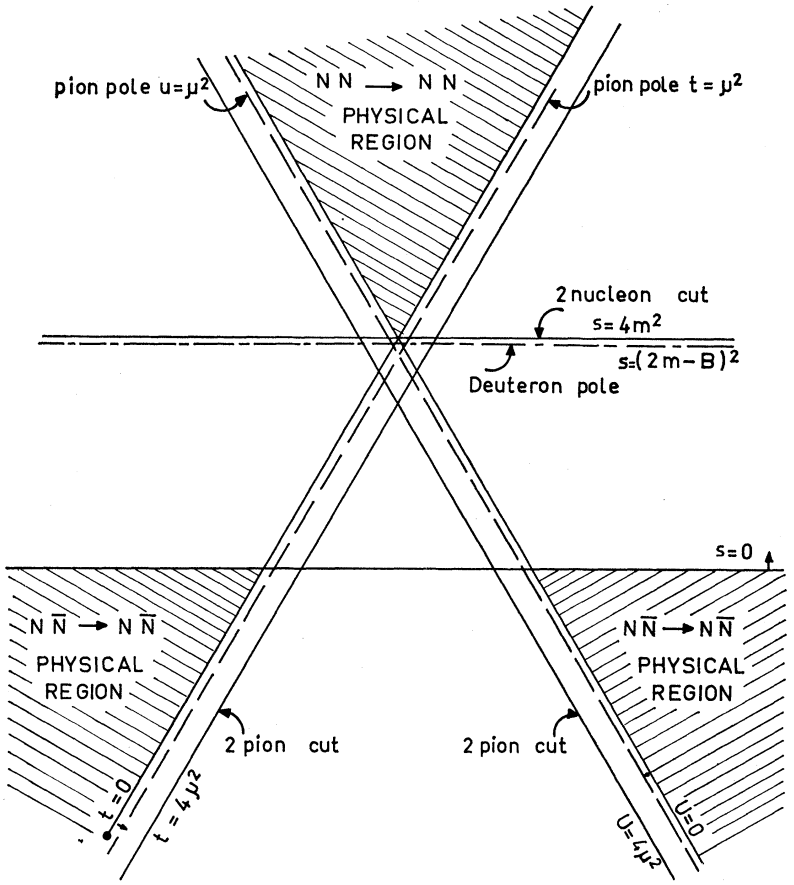


FIG. 1. Analytic properties of the Mandelstam amplitudes $F_i^I(s,t,u)$ for nucleon-nucleon scattering.

$$\mathcal{T}=[F_1^0(S-\tilde{S})+F_2^0(T+\tilde{T})+F_3^0(A-\tilde{A})+F_4^0(V+\tilde{V})+F_5^0(P-\tilde{P})]\mathcal{P}_0+[F_1^1(S-\tilde{S})+F_2^1(T+\tilde{T})+F_3^1(A-\tilde{A})+F_4^1(V+\tilde{V})+F_5^1(P-\tilde{P})]\mathcal{P}_1. \quad (3.1)$$

We refer the reader to Appendix B 3 for the precise definition of the Fermi invariants $S$, $V$, $T$, $A$, $P$ and $\tilde{S}$, $\tilde{V}$, $\tilde{T}$, $\tilde{A}$, $\tilde{P}$. The operators $\mathcal{P}_0$ and $\mathcal{P}_1$ are the isospin projectors.

The $F_i^I$ are scalar analytic functions of the Mandelstam invariants $s$, $t$, and $u$, where $s$ is the square of the total energy in the c.m. system of the two nucleons, and $t$ and $u$ refer to the annihilation channels. (See Appendix B 2 for the precise definition of those invariants.) The reason for writing the amplitude in the form (3.1) is that the Pauli principle reads simply

$$F_i^I(s,t,u)=(-)^{i+I}F_i^I(s,u,t). \quad (3.2)$$

The analytic properties of the amplitudes $F_i^I(s,t,u)$ are shown in Fig. 1 (if one assumes the validity of the Mandelstam representation). In this figure we see the pion pole, the two-pion cuts, the deuteron pole, and the two-nucleon cuts. It is always possible to single out the contribution of the pole term corresponding to the existence of a pseudoscalar particle (pion) in the $t$ and $u$ channels; the result is

$$\mathcal{T}_{(1\text{ pion})}=-3g^2\left(\frac{P}{t-\mu^2}+\frac{\tilde{P}}{u-\mu^2}\right)\mathcal{P}_0+g^2\left(\frac{P}{t-\mu^2}-\frac{\tilde{P}}{u-\mu^2}\right)\mathcal{P}_1. \quad (3.3)$$

In fact, this formula is very general, because when the nucleons are on the mass shell, it is easy to see that the form factors $NN\pi$, appearing in Fig. 2, involve only the $P$ invariant.

The total amplitude is now

$$\mathcal{T}=\mathcal{T}_{(1\text{ pion})}+\mathcal{T}_R, \quad (3.4)$$

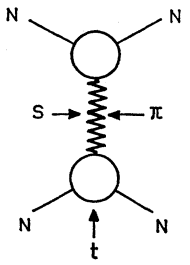


FIG. 2. One-pion intermediate-state diagram in $N$-$N$ scattering.

where $\mathcal{T}_R$ has the general form (3.1), but the corresponding $\bar{F}_i{}^I(s,t,u)$ no longer have the pion pole.

As a consequence of Eq. (3.3), we find (see Appendix D 1) that the one-pion contribution gives the wrong threshold behavior to the following:

(1) the $^1S_0$ wave, which behaves like $p^3$ instead of $p$ (where $p$ is the c.m. momentum),

(2) the $f_{J-1,J-1}$ component of the coupled triplet (in both isospins), which behaves like $p^{2J+1}$ instead of $p^{2J-1}$. (Among these amplitudes is $^3S_1$, the $s$-wave deuteron amplitude.)

The reason for this strange behavior is very simple: The one-pion contribution has *more symmetry* than the total amplitude, which gives independent contributions to all $S$, $V$, $T$, $A$, $P$ invariants. Thus the partial waves are not independent in the one-pion exchange approximation, and one finds, for instance,

$$(^1S_0)_{(1\text{ pion})} = -(^3P_0)_{(1\text{ pion})}. \tag{3.5}$$

This relation explains why the one-pion contribution to the $^1S_0$ wave behaves like a $p$ wave.

In particular, we notice that for the two $s$ waves $^3S_1$ and $^1S_0$, *the one-pion contribution gives a p-wave threshold behavior, and this fact is model independent.* The nucleon-nucleon systems are a physical example in which the "nearest singularity" (the pion pole in dispersive language) is *not* the dominant one for these waves. The consequence is that any relativistic model which can be expected to give the $s$-wave phase shift quantitatively must necessarily include a sophisticated description of the two-pion (and also three-pion) forces, because the one-pion forces have negligible effects on those waves at low energy.[18,19]

### B. Particular Features of [1,1] Approximation

From the partial-wave Born series

$$f^{J,T}(s) = \alpha f_{B1}{}^{J,T}(s) + \alpha^2 f_{B2}{}^{J,T}(s) + \cdots, \tag{3.6}$$

where $\alpha = g^2/4\pi$ is the renormalized coupling constant, we construct the first approximation:

$$[1,1]^{J,T}(s) = \alpha f_{B1}{}^{J,T}(s) \times [f_{B1}{}^{J,T}(s) - \alpha f_{B2}{}^{J,T}(s)]^{-1} f_{B1}{}^{J,T}(s), \tag{3.7}$$

where the $f_{Bn}{}^{J,T}(s)$ are in general $2\times 2$ noncommuting matrices. For more details and for the connection between the $f$'s and the phase shifts, see Appendix C 2. The relations between the partial-wave amplitude $f^{J,T}(s)$ and the invariant amplitude (3.1) are given in GGMW, and are quoted in Appendix C1.

The complete computation of the Feynman diagrams up to fourth order is given in Appendix C; these calculations have been performed, with different methods, by Gupta *et al.*[20] and by Wortman.[21] From these computations, one deduces the first and second Born terms necessary to build up the [1,1] Padé approximant.

We come now to the problem of knowing if all the partial-wave amplitudes will have the correct threshold behavior in our theory. It is shown in Appendix D 2 that this is the case for all waves, with exception of the $^1S_0$ singlet: This wave, in the [1,1] Padé approximation, has the anomalous pathological threshold behavior of a $d$ wave; this is because the first Born term itself had a wrong threshold behavior. Our theory being a low-energy one, its predictions about this wave are meaningless; we conclude that, in order to treat the $^1S_0$ wave by the Padé method in the framework of the assumed Lagrangian, one has to compute at least the [2,1] or the [1,2] approximant, both of which involve terms of the sixth perturbative order.

In regard to the other waves which have a pathological behavior for the first Born term (among which is the $s$ wave of the deuteron), it is remarkable that the first Padé approximation restores the correct threshold behavior.

## IV. BOUND-STATE PROBLEM

Let us first recall the well-known structure of the bound and antibound (virtual) states in the nucleon-nucleon system: There is a bound state (the deuteron) in the $J=1$ coupled triplet, with a binding energy $B=2.225$ MeV; and an antibound state in the $^1S_0$ singlet with an antibinding energy of 38 keV. No bound or antibound states exist in any other wave.

Let us now discuss these points in detail, in the framework of our approximation. The bound-state equation reads [taking into account Eq. (3.7)]

$$\det[f_{B1}{}^{J,T}(s) - \alpha f_{B2}{}^{J,T}(s)] = 0. \tag{4.1}$$

Equation (4.1) is of first degree in $\alpha$ for the singlet and the uncoupled triplet; for the coupled triplet it is of second degree in $\alpha$. Giving to $\alpha$ its physical value, we look for the zeros of (4.1) in $s$. [It may be technically easier in some cases to compute $\alpha=\alpha(s)$ from (4.1) and then intersect this curve with the physical value of $\alpha$.] The bound states are to be selected among those zeros.

The antibound-state equation reads

$$\det\{f_{B1}{}^{J,T}(s) - \alpha f_{B2}{}^{J,T}(s) + i\alpha[f_{B1}{}^{J,T}(s)]^2\} = 0. \tag{4.2}$$

This last equation is obtained by noticing that

$$\begin{aligned} f_{B1}{}^{J,T}(s_{II}) &= f_{B1}{}^{J,T}(s_I), \\ f_{B2}{}^{J,T}(s_{II}) &= f_{B2}{}^{J,T}(s_I) - i[f_{B1}{}^{J,T}(s_I)]^2. \end{aligned} \tag{4.3}$$

Equations (4.3), which express the second-sheet values of $f_{B1}$ and $f_{B2}$ as functions of their first-sheet values, are

[18] H. P. Stapp, T. J. Ypsilantis, and N. Metropolis, Phys. Rev. **105**, 302 (1957).

[19] J. S. Ball, A. Scotti, and D. Y. Wong, Phys. Rev. **142**, 1000 (1966).

[20] S. N. Gupta *et al.*, Phys. Rev. **138**, B1500 (1965).

[21] W. R. Wortman (private communication); Phys. Rev. **176**, 1762 (1968).

trivially deduced from the elastic unitarity condition written for the perturbative Born series.

Let us begin the discussion with the bound states. The well-known analytical structure in $s$ of the partial-wave amplitudes in the nucleon-nucleon scattering is the following:

(1) the right-hand cut starting at $s=4m^2$ (elastic cut); then, superimposed, the first inelastic cut at $s=(2m+\mu)^2$; and so on.

(2) the left-hand cut starting at $s=4m^2-\mu^2$ (1 pion cut); then superimposed, the two-pion left-hand cut starting at $s=4m^2-4\mu^2$; and so on.

Between those two cuts is a region of analyticity:

$$4m^2-\mu^2<s<4m^2. \tag{4.4}$$

In this gap the $S$ matrix is real (time-reversal invariance); that is, our $f_{Bn}{}^{J,T}(s)$ are purely imaginary.

We notice that it is found experimentally that the binding energy of the deuteron is 2.225 MeV; this will correspond to a pole which sits in the gap approximately half-way between the right- and left-hand cuts. After those generalities, we come now to the discussion of the roots of (4.1). We remark that our Eqs. (4.1) reduce for the singlet and uncoupled triplet to

$$\alpha=f_{B1}{}^{J,T}(s)/f_{B2}{}^{J,T}(s)\equiv\alpha(s). \tag{4.5}$$

The function $\alpha(s)$ is real when $s$ is in the gap, as noticed previously. Let us forget about spin and isospin complications; then the Froissart-Gribov integrals giving $f_{Bn}(s)$ read

$$\begin{aligned}(n\neq 1)\quad f_{Bn}{}^{J}(s)&=\frac{8}{\pi(s-4m^2)}\int_{4\mu^2}^{\infty}\mathrm{Abs}_t{}^{(n)}(s,t')\\&\quad\times Q_J\left(1+\frac{2t'}{s-4m^2}\right)dt',\\ f_{B1}{}^{J}(s)&=\frac{8}{\pi(s-4m^2)}\int\delta(t'-\mu^2)\\&\quad\times Q_J\left(1+\frac{2t'}{s-4m^2}\right)dt'\\&=\frac{8}{\pi(s-4m^2)}\;Q_J\left(1+\frac{2\mu^2}{s-4m^2}\right).\end{aligned} \tag{4.6}$$

We see that when $s$ varies in the gap (4.4), $f_{B1}{}^{J}(s)$ varies from zero (when $s=4m^2$) to infinity (when $s=4m^2-\mu^2$) while all the others $f_{Bn}{}^{J}(s)$ vary from zero to a finite value. We see once more that the first Born term, which was singular from the algebraic point of view, is also singular from the analytical point of view, becoming infinite (logarithmically) at the point $s=4m^2-\mu^2$.

As a consequence the function $\alpha(s)$ of formula (4.5) varies from a certain value $\alpha(4m^2)$ to infinity when $s\to 4m^2-\mu^2$. The value of $\alpha(s)$ at threshold has a remarkable property: It increases *exponentially* with $J$. The reason is simple: $\mathrm{Abs}_t{}^{(n)}(s,t')$ will be peaked around some value $t_c>4\mu^2$; then

$$\alpha(s)\underset{s\approx 4m^2}{\sim}\frac{Q_J(1+2\mu^2/(s-4m^2))}{Q_J(1+2t_c/(s-4m^2))}\sim\left(\frac{t_c}{\mu^2}\right)^{J+1}. \tag{4.7}$$

All these results are not modified by the presence of spin and isospin. In fact Figs. 3 and 4 show this clearly; in $T=0$ the singlet and uncoupled triplet have $\alpha(s)$ always negative, while in $T=1$ they have $\alpha(s)$ always positive (the shape of the curves for $T=1$ is much the same as for $T=0$, except that they are upside down), but one sees that $\alpha(s)$ increases with $J$, and stays in all cases far above the physical value 15.

For the coupled triplet nothing is essentially changed, and one finds that the two roots $\alpha_+$ and $\alpha_-$ of the second-degree equation (4.1) are always real in the gap, that both tend to infinity for $s\to 4m^2-\mu^2$, and that they are of opposite sign. One sees in Figs. 5 and 6 that $\alpha(s)$ increases exponentially with $J$, and that only the wave $J=1$ gives rise to a bound state for $g^2/4\pi=15$; the binding energy is found to be 4.8 MeV, so we find that in the gap only the $s$ waves can give rise to a pole of the $S$ matrix when the coupling constant has its physical value.

In the same way, antibound states, which are second-sheet poles of the $S$ matrix lying in the gap (4.4), can be studied. It is found that for the $J=1$, $T=0$ coupled triplet the two roots of (4.2) are always real and opposite in sign and that the positive one is always less than 3.5, so no antibound states are found in this $s$ wave. With regard to the $^1S_0$ $s$ wave: As already explained, this wave has pathological $d$-wave behavior at the origin, and therefore no reliable results can be drawn.[22–27]

The reader may be astonished by the fact that when the coupling constant goes to infinity, the pole of the $S$ matrix which is in the gap tends to the left-hand cut. One might suppose that there are examples in which the bound state sits on the left-hand cut. (The case of $^4$He, however, gives rise to anomalous cuts which cover the gap entirely, so in such an example there is no more gap.) We want to point out that in the relativistic case, the bound state has to be between $s=0$ and $s=4m^2$, because otherwise for $s<0$ it will appear as a pole in the physical regions of the crossed channels. This is not so for nonrelativistic theories in which when the coupling constant tends to infinity, the binding energy does also.

---

[22] M. H. MacGregor, R. A. Arndt, and R. M. Wright, Phys. Rev. **141**, 873 (1966); **169**, 1128 (1968); R. E. Seamon *et al.*, *ibid.* **165**, 1579 (1968).

[23] F. J. Dyson and N. H. Xuong, Phys. Rev. Letters **13**, 815 (1964).

[24] R. A. Arndt, Rev. Mod. Phys. **39**, 710 (1967).

[25] A. Scotti and D. Y. Wong, Phys. Rev. **138**, B145 (1965).

[26] J. L. Basdevant and B. W. Lee, CEN-Saclay, Report (unpublished); S. Caser, C. Piquet, and J. L. Vermeulen, Nucl. Phys. **B14**, 119 (1969).

[27] J. L. Basdevant and B. W. Lee, Phys. Letters **29B**, 437 (1969).

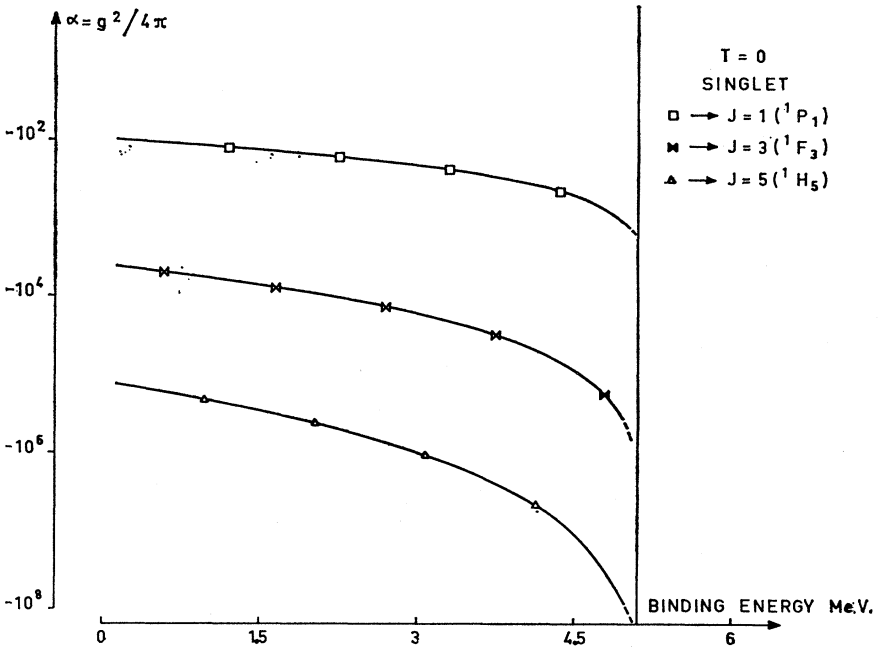


FIG. 3. Coupling constant $\alpha=g^2/4\pi$ versus the bound-state binding energy for the $T=0$ singlet.

One can show that all $[N,N]$ approximants have a root $\alpha$ which tends to infinity when $s$ tends to the left-hand cut. (This is so because the first Born term becomes infinite at the same time.) Clearly this is a defect of the model, because there is no reason why the bound state cannot approach continuously the region $0<s<4m^2-\mu^2$. However, this is a minor defect, for the following reason: If one computes the $s$-wave bound states in potential scattering for the potential $Ge^{-\mu r}/r$ (for which Padé convergence can be proved[28]), then it is true that the same defect will occur in every finite-order approximation. Nevertheless, the "weak" (logarithmic) singularity at $s=4m^2-\mu^2$, will become more and more washed out as the order of approximation increases. For an enlightening discussion on this point, we refer the reader to Ref. 26.

It is clear that we can trust the position of the pole if it is sufficiently far away from the left-hand cut. In

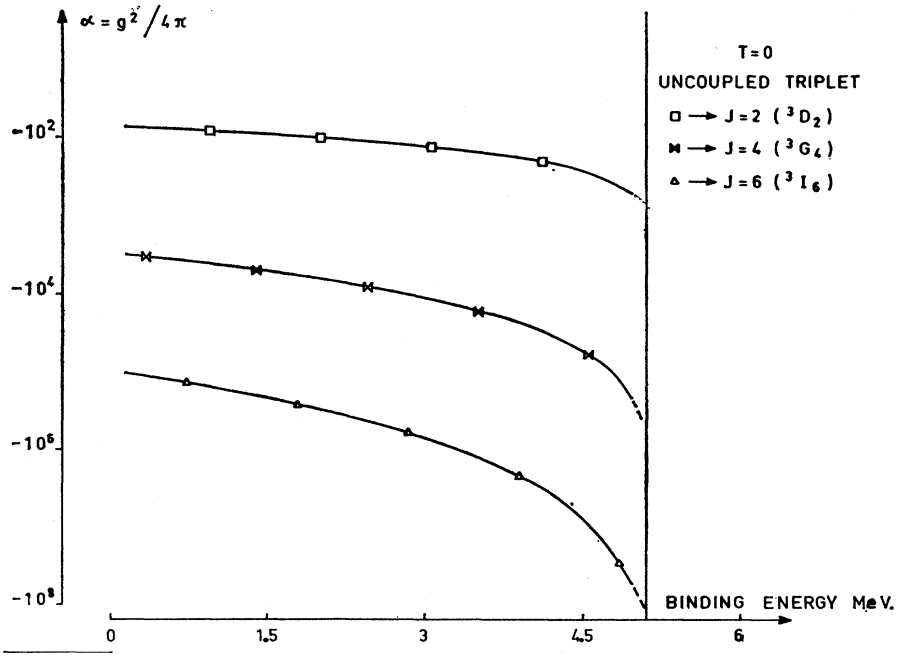


FIG. 4. Coupling constant $\alpha=g^2/4\pi$ versus the bound-state binding energy for the $T=0$ uncoupled triplet.

[28] C. R. Garibotti and M. Villani, Nuovo Cimento 59A, 107 (1969); 61A, 747 (1969).

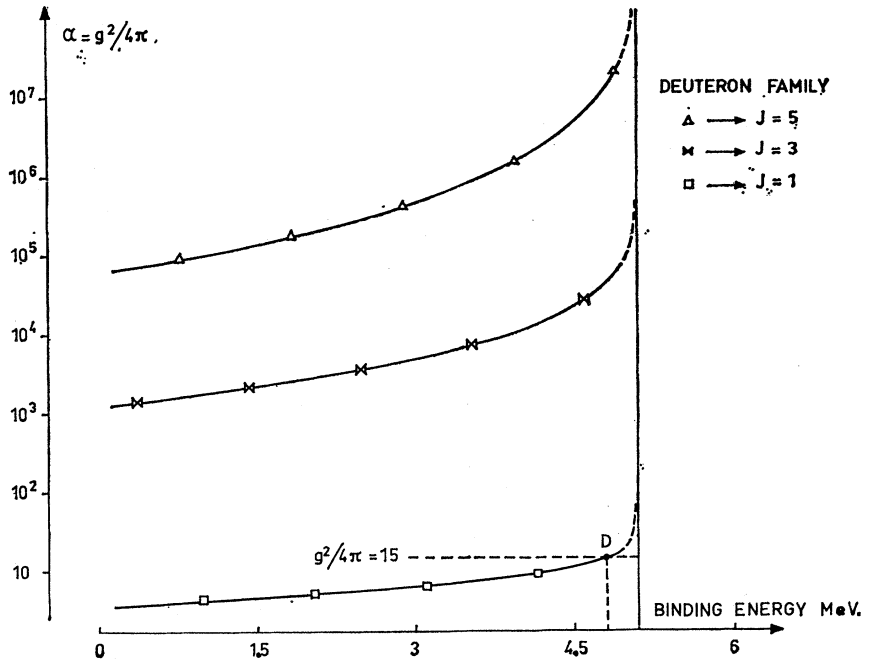


FIG. 5. Coupling constant $\alpha = g^2/4\pi$ versus the bound-state binding energy for the deuteron family.

our case, however, the pole comes very near to the left-hand singularity for the physical value of $\alpha$, and this limits the reliability of the binding energy one can deduce.

We now come to the question of the possibility of finding poles for $\alpha$ real and $(\mathrm{Re}s) < 4m^2 - \mu^2$, and of understanding their physical meaning. In fact, for the $J=1$ coupled triplet one finds, for $\alpha = 15$, two poles at $4m^2 - s = (3.5 \pm i4.2)\mu^2$. These poles have large imaginary part and have a real part which is already far from the beginning of the left-hand cut. It seems reasonable therefore, not to interpret them as bound states, but rather as unphysical singularities contributing to the left-hand cut.

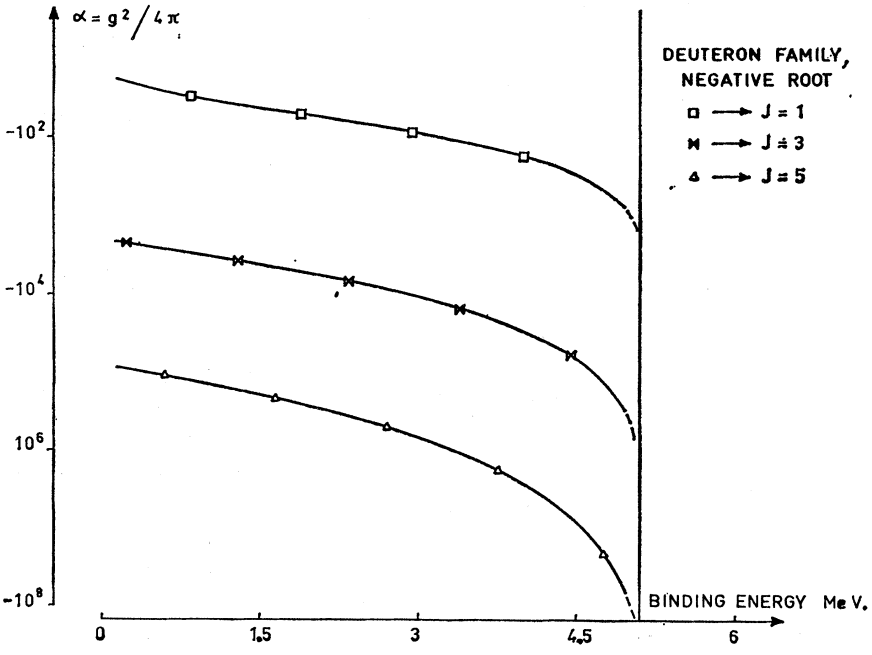


FIG. 6. Coupling constant $\alpha = g^2/4\pi$ versus the bound-state binding energy for the deuteron family (negative root).

## V. DEUTERON

We shall now compute some physical quantities connected with the deuteron, which will enable us to perform a careful analysis of our results.

The deuteron appears as a bound state of the coupled triplet amplitude for $J=1$ and $T=0$, described by the $S$ matrix

$$S^{J=1,T=0}(s)=I+if^{J=1,T=0}(s), \tag{5.1}$$

where $I$ is the $2\times2$ unit matrix, and $f^{J=1,T=0}(s)$ is

$$f^{J=1,T=0}(s)=\begin{bmatrix} f_S(s) & f_{SD}(s) \\ f_{SD}(s) & f_D(s) \end{bmatrix}. \tag{5.2}$$

This last matrix is analytic in $s$ (the square of the total c.m. energy), and has a pole for $s=m_D{}^2$. In the vicinity of this pole, (5.2) becomes

$$f^{J=1,T=0}(s)\approx\begin{bmatrix} R_S & R_{SD} \\ R_{SD} & R_D \end{bmatrix}\Big/(s-m_D{}^2). \tag{5.3}$$

The theorem of factorization of residues tells us that

$$R_{SD}{}^2=R_SR_D. \tag{5.4}$$

As shown in Appendix D 3, those residues are connected to useful physical quantities. In particular, we have

$$\rho=\tan\epsilon_D=-R_{SD}/R_S, \tag{5.5}$$

where $\epsilon_D$ is the mixing angle; and

$$\rho(-B,-B)=\frac{1}{(mB)^{1/2}}+i\frac{16(mB)^{1/2}}{R_S+R_D}, \tag{5.6}$$

where $m$ is the nucleon mass, $B$ is the deuteron binding energy, and $\rho(-B,-B)$ is the deuteron effective range. [The reader is referred to the paper of Hulthén and Sugawara[4] for the definition of $\rho$ and $\rho(-B,-B)$.] By means of those two quantities, one can calculate the physical quantities related to the deuteron, such as quadrupole moment or magnetic moment (at least in first approximation). To represent a bound state it is necessary that the residues $R_S$ and $R_D$ be purely imaginary with a *negative imaginary part.*

We notice that our Padé approximation will automatically satisfy the factorization of residues, and will also be Hermitian. It is then only necessary to check that the sign of the imaginary part of $R_S$ is negative, which is the case. Moreover, when $\alpha=14.7$, which implies a binding energy of 4.8 MeV for our pole, we get

$$\tan\epsilon_D=0.006.$$

The experimental value is 0.03, so our result is too small by a factor of 5. However, we notice that the sign of the quadrupolar electric moment will be right. It then follows that the sign of the scattering mixing angle will also be right (see Appendix D 3). Therefore, the pole we find in the $S$ matrix really has the physical characteristics of the deuteron. For the effective range a negative value is obtained. We postpone the discussion of all this to Sec. VII, which is devoted to phase shifts.

## VI. REGGE TRAJECTORIES

Once we have found a zero of the denominator of an approximant for integer $J$, there are no difficulties in following it by continuity in the complex $J$ plane. It is in this way that the corresponding Regge trajectory is determined.

A first rising trajectory is observed in the $T=0$ coupled triplet amplitude, i.e., the deuteron trajectory. Looking at Fig. 7, one sees that this trajectory crosses the physical value $J=3$ near 300 MeV ($T_{\text{lab}}$). However, the imaginary part of the trajectory is so large at this energy that it cannot correspond to any physical particle (resonance) which one could identify as the Regge recurrence of the deuteron.

A second rising Regge trajectory is observed in the $T=1$ singlet amplitude. Looking at Fig. 8, it can be seen that it gives rise to narrow resonances in the ${}^1D_2$ and ${}^1G_4$ waves near 90 and 380 MeV ($T_{\text{lab}}$), respectively. Its extrapolation down to $J=0$ gives rise to a bound state comparable with the one we obtain in the ${}^1S_0$ state. So (quite surprisingly), although the ${}^1S_0$ wave does not Reggeize, the extrapolation (graphical only) down to $J=0$ of the Carlsonian sequence of the associated waves gives back approximately the same "bound state." It seems to us very important to see if in an improved version of this work—involving higher orders, for instance—this peculiarity is confirmed. If such is the case, it would be, in this model, some confirmation of the so-called "principle of nuclear democracy."

Of course, the values found for the energies of the resonances ${}^1D_2$ and ${}^1G_4$ are necessarily only indicative (if one remembers, for instance, that our deuteron is too strongly bound) in the present state of the model. However, their existence, at least, has been already suggested by some authors.[23,24] A more complete discussion of these resonances is given in the following section.

## VII. PHASE SHIFTS

Since there exist several accurate phase-shift analyses of nucleon-nucleon elastic and even inelastic scattering (up to 750 MeV for $T_{\text{lab}}$),[22] we have computed all the phase shifts predicted by our theory (with the exception, as explained previously, of the ${}^1S_0$ phase shift).

As already stated, our theory is a low-energy one. Strictly speaking, it should be reliable up to an energy corresponding to the first inelastic threshold encountered, i.e., up to $T_{\text{lab}}=280$ MeV, which corresponds to the production of one pion (remember that at the order we are dealing with, no inelastic branch points appear in the perturbation series). Since, how-

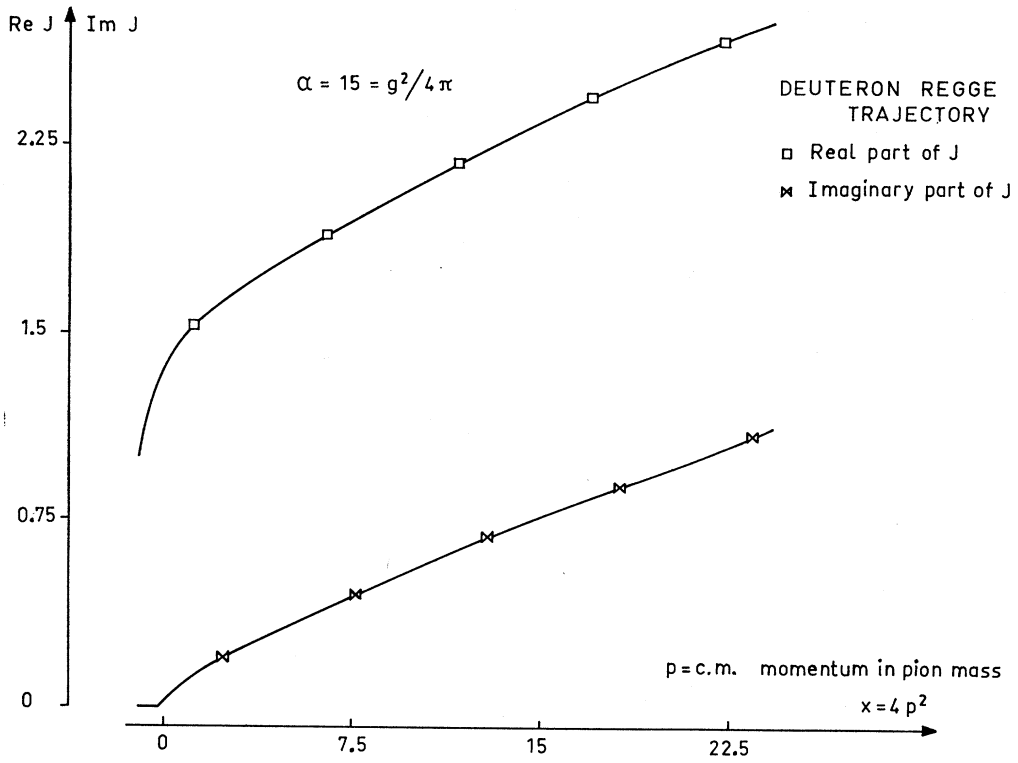


FIG. 7. The deuteron Regge trajectory.

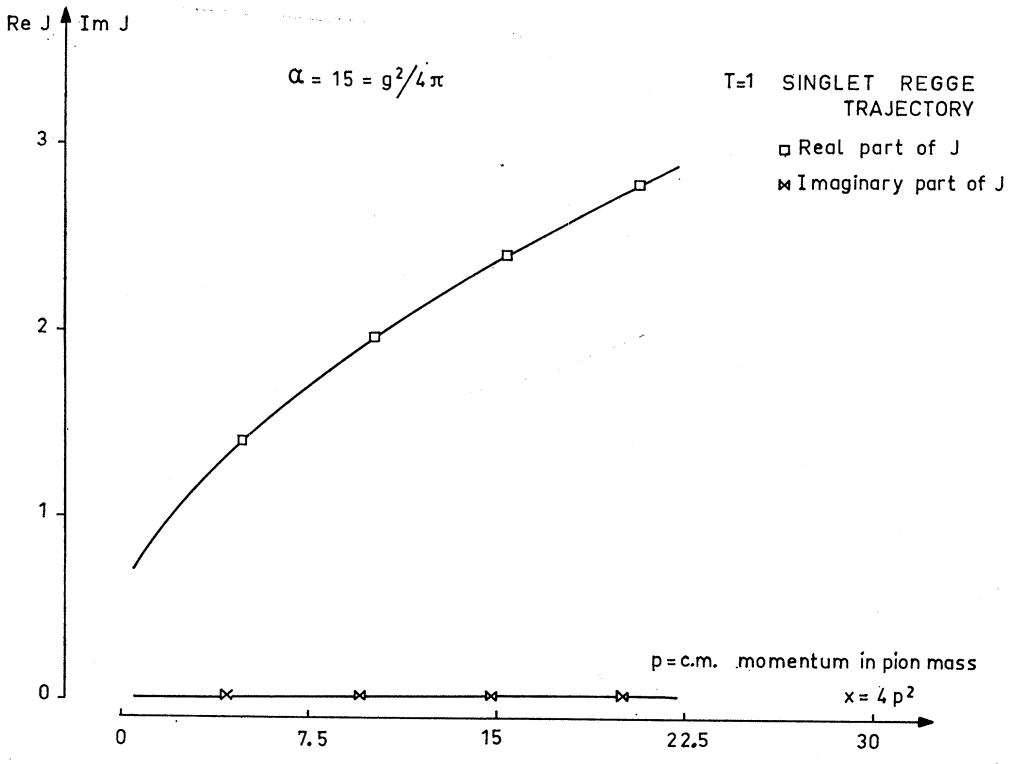


FIG. 8. The $T=1$ singlet Regge trajectory.

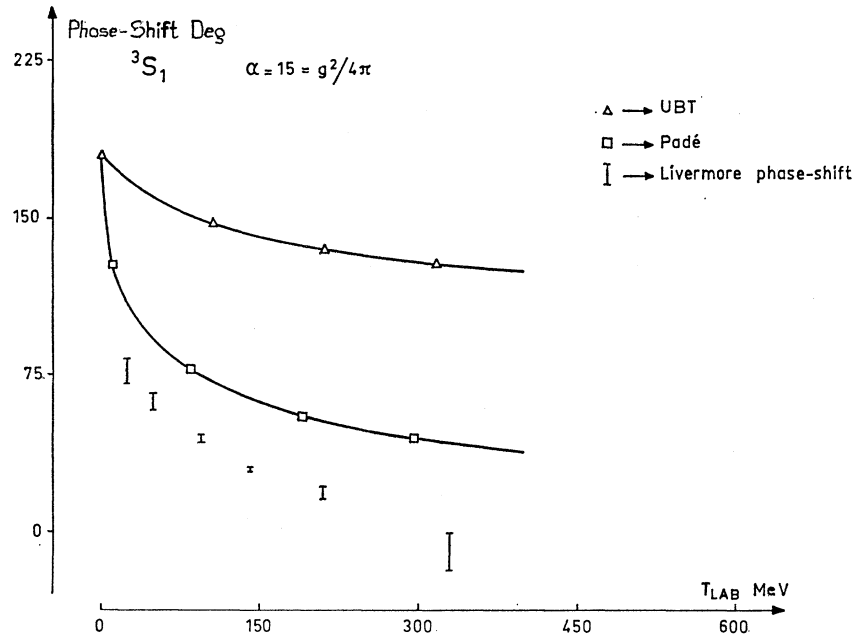


FIG. 9. Comparison between the experimental phase shifts, the unitarized Born term, and the Padé solution for the $^3S_1$ phase shift.

ever, the inelasticity effects are small up to 400 MeV, we should be able to reproduce the analysis up to this energy, at least for higher partial waves. Moreover, it is just in this energy range that the experimental fits are the most reliable.

In Figs. 9–20 we have plotted the calculated phase shifts, compared with the fixed-energy data of Ref. 22 and with the phase shifts predicted on the basis of the so-called "unitarized Born term" (UBT); the pion-nucleon coupling constant is held fixed at $\alpha = 15$. In Figs. 21–27 we have plotted the phase shifts obtained assuming $\alpha = 10$, 15, and 20. This has been done because, even if the essential parameter in our theory is known, it is interesting to look at how sensitive the results are to its variation.

Looking at all these figures, it can be noticed that (with the exception of $^1D_2$ and $^1G_4$ waves, which will be discussed later) the qualitative agreement with the

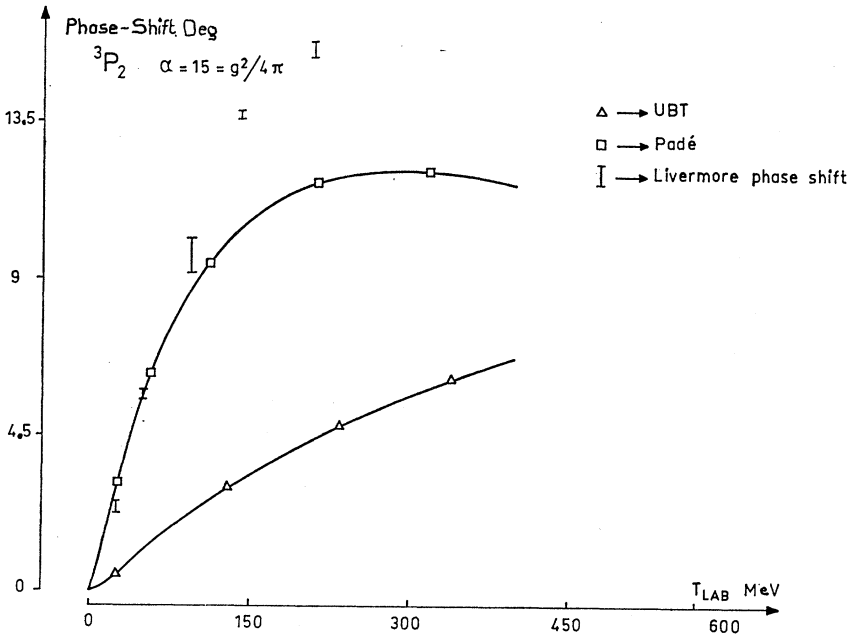


FIG. 10. Comparison between the experimental phase shifts, the unitarized Born term, and the Padé solution for the $^3P_2$ phase shift.

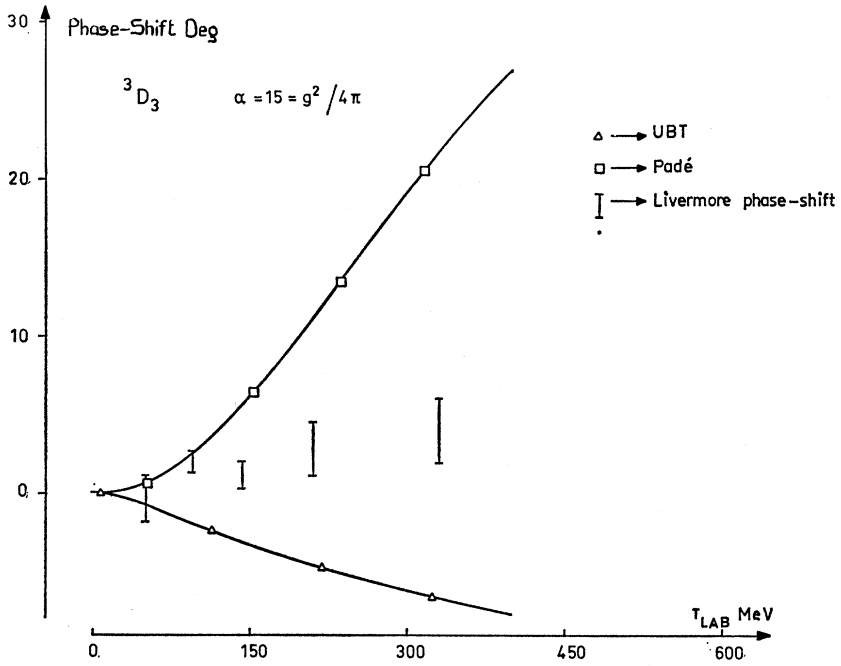


FIG. 11. Comparison between the experimental phase shifts, the unitarized Born term, and the Padé solution for the $^3D_3$ phase shift.

data is always good. All the signs of the phase shifts are correct, at least at very low energy. This means that we predict correctly the sign of the two-nucleon forces.

The comparison with UBT is perhaps not completely meaningful from a theoretical standpoint; we make it because UBT is the simplest possible model, and always, when a new theory is proposed, the comparison with the Born term should be made as a first simple test. Now, let us first remark that since all the $l=J-1$ coupled triplet waves of UBT behave wrongly at threshold, they cannot reproduce the data, whereas our model does not present this defect. Furthermore, looking at Fig. 11, we see that the sign of the $f_{l=J-1}$ phase shifts in $T=0$ is wrong for UBT and correct for the present theory. To summarize, for all waves of this family (i.e., the $l=J-1$ coupled triplet waves), the agreement with data is much better in the present theory than in UBT (see Figs. 9, 10, and 12).

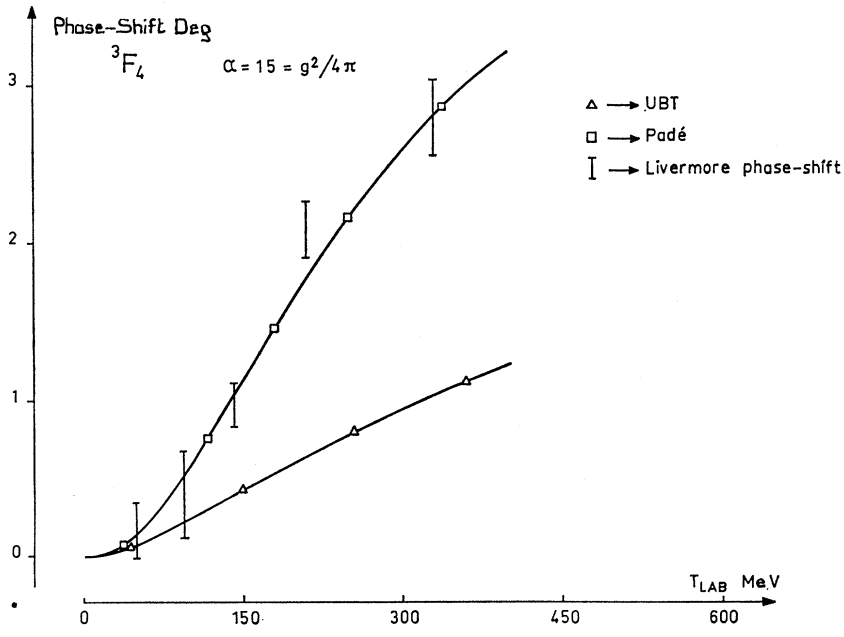


FIG. 12. Comparison between the experimental phase shifts, the unitarized Born term, and the Padé solution for the $^3F_4$ phase shift.

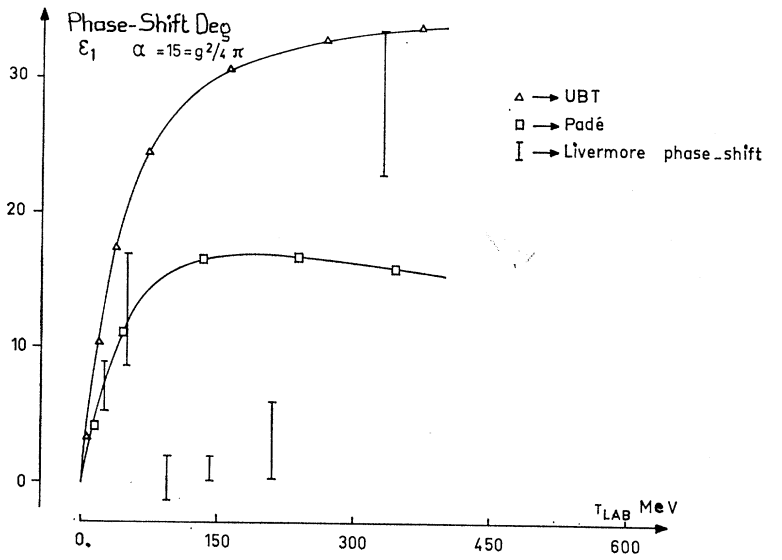


FIG. 13. Comparison between the experimental phase shifts, the unitarized Born term, and the Padé solution for the $\epsilon_1$ phase shift.

If we parametrize the behavior of the ${}^3S_1$ phase shift by an effective-range formula, we obtain

$$a = 2.82 \text{ F for the scattering length},$$

$$r = 0.9 \text{ F for the effective range}.$$

(Experimentally, $a = 5.37$ F and $r = 1.73$ F.) As mentioned previously, the effective range can be obtained in terms of the parameters of the deuteron pole by means of Eq. (5.6). If we identify the pole we find at $B = 4.8$ MeV with the deuteron, we obtain a negative value

$$\rho(-B, -B) = -5.08 \text{ F}.$$

We explain this inversion of the sign in the following way: $r$ and $\rho(-B, -B)$ have to coincide if the Jost functions can be well approximated only with the bound-state pole. This is the case if it lies near threshold. However, in our case, the pole lies near the left-hand cut; moreover, there exists a pair of complex conjugate poles so that a good approximation of the Jost functions must take into account not only the real pole but also the couple of complex ones. When such a procedure is carried out carefully, the resulting values for $a$ and $r$ are the same as those quoted above.

The preceding analysis shows that there is no in-

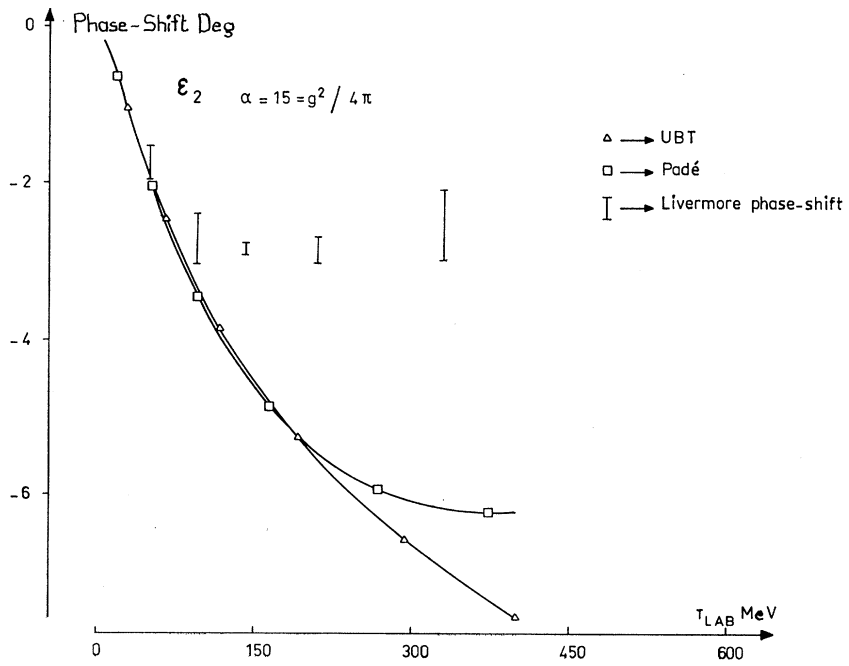


FIG. 14. Comparison between the experimental phase shifts, the unitarized Born term, and the Padé solution for the $\epsilon_2$ phase shift.

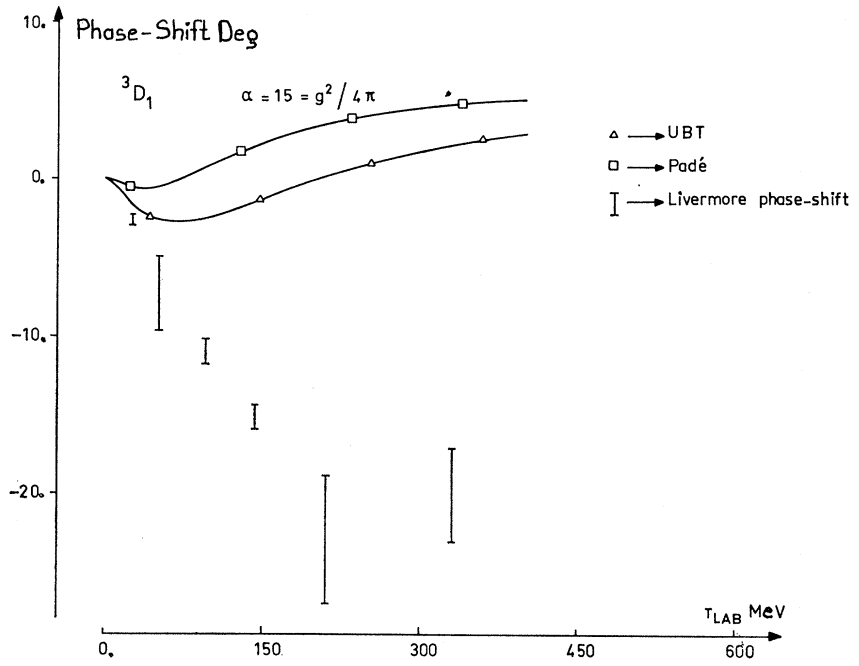


FIG. 15. Comparison between the experimental phase shifts, the unitarized Born term, and the Padé solution for the $^3D_1$ phase shift.

compatibility between the phase shifts predicted by the present theory and the experimental ones. It is interesting to examine how the phase shifts change when the coupling constant $\alpha$ is allowed to vary. With $10 \leq \alpha \leq 20$, the experimental data are generally well reproduced in partial waves with $J > 1$ (see Figs. 21–27). For $J = 1$ we notice that the coupled triplet phase shifts are stable with respect to the variation of $\alpha$ (see Figs. 21 and 24). We come now to the discussion of the $^1D_2$ and $^1G_4$ phase shifts. As we have already seen in discussing Regge trajectories, in our theory, these waves exhibit resonances at 81.5 and 370 MeV, respectively, for $\alpha = 15$. The widths are 4 and 6 MeV, respectively. At the energies where we find them, the presence of these resonances is incompatible with the experimental data.

The presence of a resonance in the $^1D_2$ wave has already been suggested by some authors, starting from

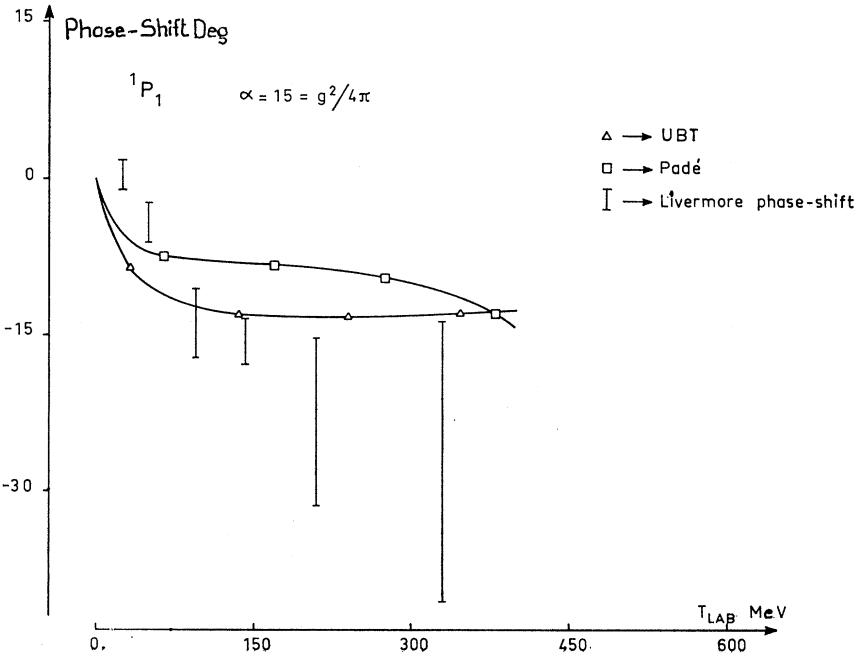


FIG. 16. Comparison between the experimental phase shifts, the unitarized Born term, and the Padé solution for the $^1P_1$ phase shift.

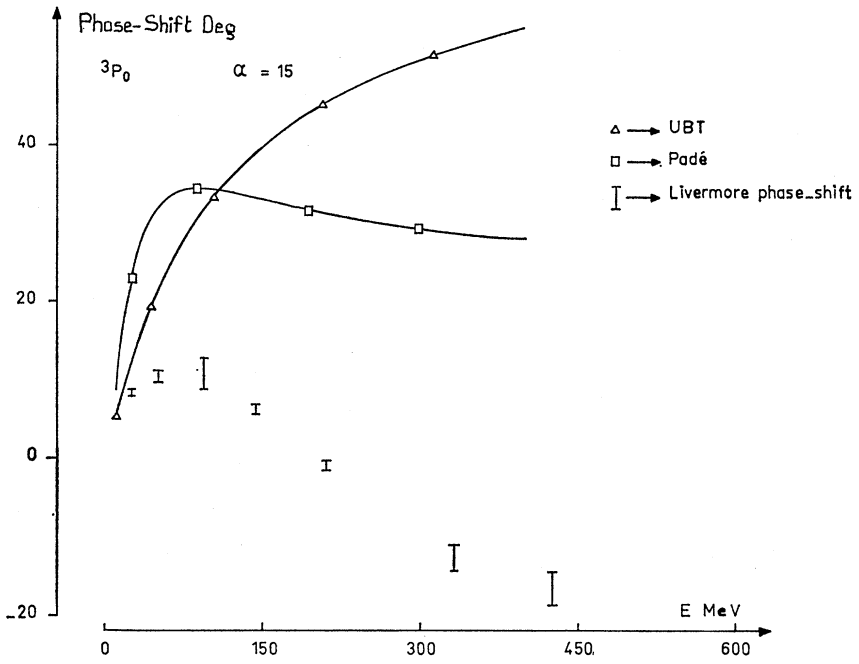


FIG. 17. Comparison between the experimental phase shifts, the unitarized Born term, and the Padé solution for the $^3P_0$ phase shift.

a different theoretical basis.[23,24] We note that if one assumes the existence of a rising Regge trajectory which interpolates the virtual singlet state, the simplest assumption for its behavior in energy is

$$J \approx r p_{\text{c.m.}}, \tag{7.1}$$

the quantity $r$ being of the order of the singlet effective range $r_s$. Such a hypothesis will give rise to resonances in the $^1D_2$ and $^1G_4$ waves. In fact, the numerical value that we obtain for $r$ is not very far from $r_s$. However, if $r$ is multiplied by a factor of 2 in Eq. (7.1), this will change the resonance energy $T_{\text{lab}}$ by a factor of 4, because

$$T_{\text{lab}} = 2 p_{\text{c.m.}}^2 / m. \tag{7.2}$$

We conclude that, although no inconsistency enters in the model, our theory cannot, at this stage, predict correctly the positions of possible higher-energy nucleon-

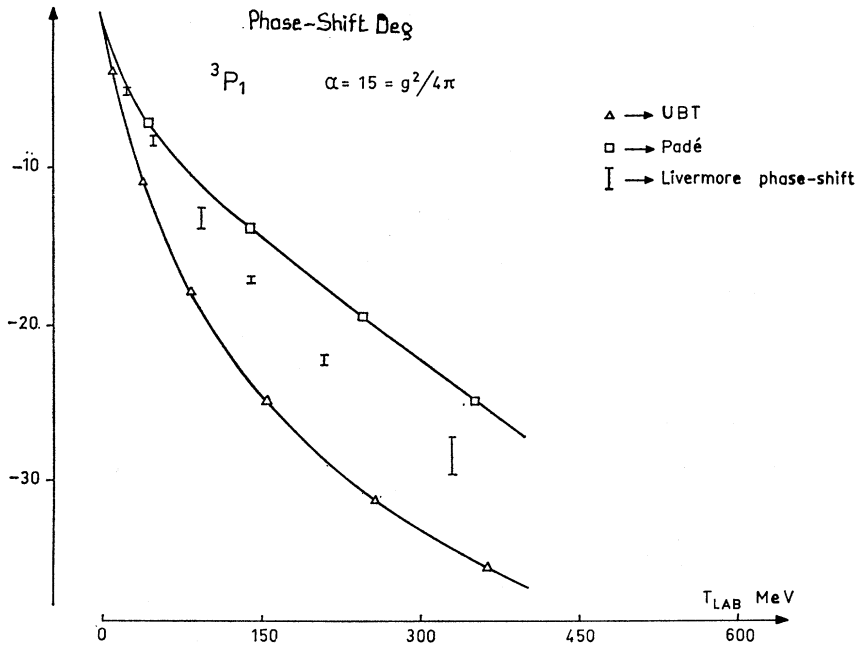


FIG. 18. Comparison between the experimental phase shifts, the unitarized Born term, and the Padé solution for the $^3P_1$ phase shift.

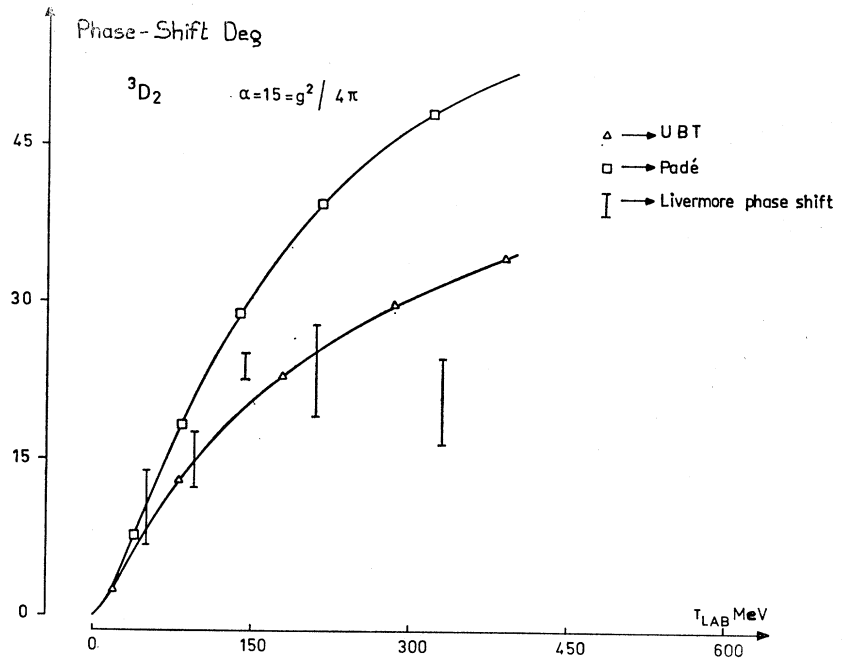


FIG. 19. Comparison between the experimental phase shifts, the unitarized Born term, and the Padé solution for the $^3D_2$ phase shift.

nucleon resonances. We think, however, that at this stage the prediction of the existence of these resonances is meaningful.

## VIII. DISCUSSION AND CONCLUSIONS

As we have seen, our model seems to work nicely, in view of the fact that (i) we have only considered the lowest-order unitary Padé approximation, (ii) there are no free parameters left, and (iii) we have chosen the simplest possible Lagrangian.

Our theory is certainly satisfactory from a formal standpoint, because it allows the identification of bound states, as poles of the amplitudes, whereas the usual perturbative approach breaks down precisely at that point. One may wonder to what extent our results are consistent with the fact that we have taken into account only the pion force. In fact, in recent years,

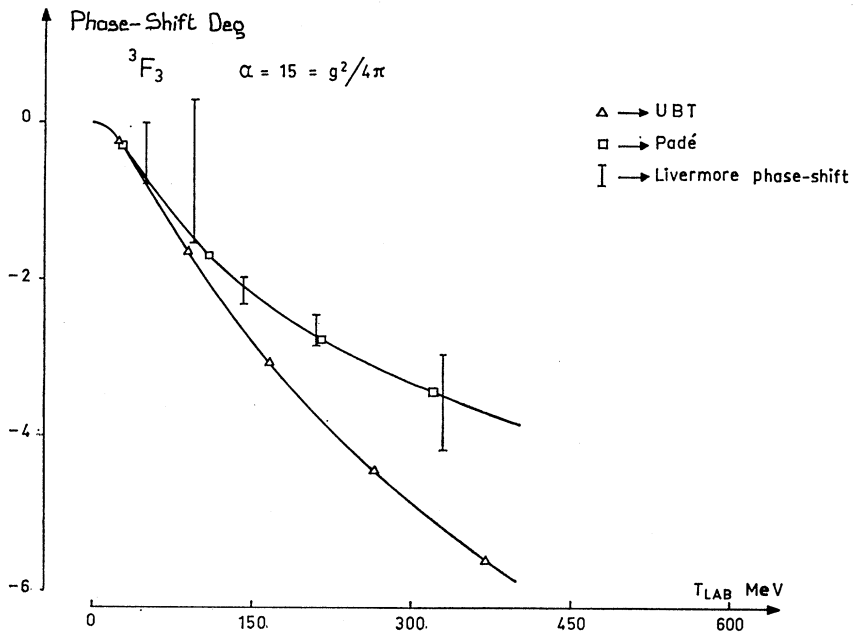


FIG. 20. Comparison between the experimental phase shifts, the unitarized Born term, and the Padé solution for the $^3F_3$ phase shift.

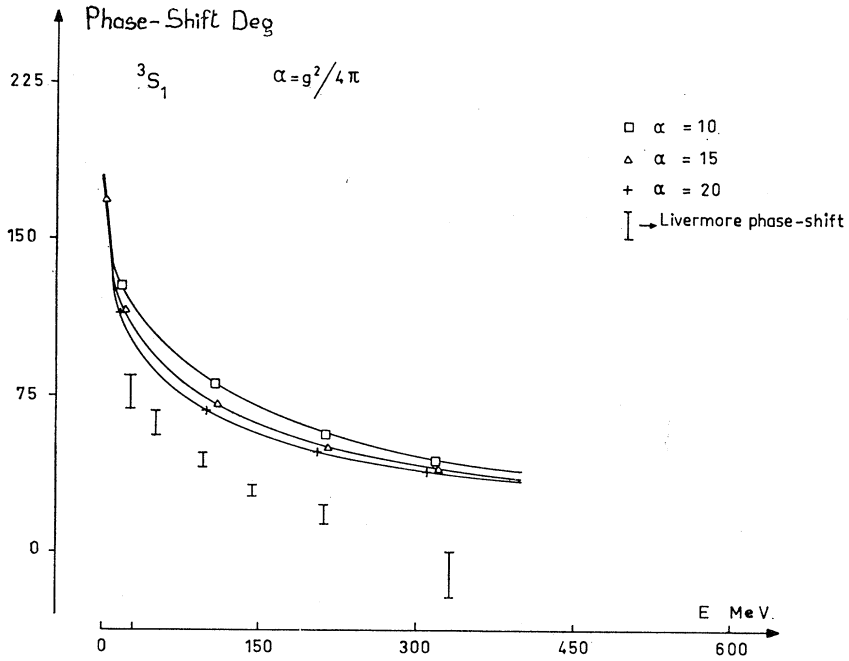


FIG. 21. Comparison between the experimental phase shifts and the Padé solution for three values of the coupling constant $\alpha = g^2/4\pi$, for the $^3S_1$ wave.

fits to nucleon-nucleon scattering have been proposed by adding vector-meson exchange to that force. This has been done in the framework of nonrelativistic potential theory, with the introduction of the so-called "one-boson-exchange potentials" (see Ref. 3 for an up-to-date review of such theories), as well as in relativistic scattering theory, using dispersion relations and the $N/D$ method,[19,25] with nice results, at least from a phenomenological point of view.

First of all, it must be said that our treatment does not exclude such forces, but that in this framework they appear only at higher orders in the perturbation series of our Lagrangian (1.1). Up to fourth order in the perturbation series these forces do not appear. Therefore, as concerns the effects of such forces, the convergence of the Padé approximants is not yet achieved in the present calculation. In fact, our method reproduces well the higher partial waves, whereas UBT

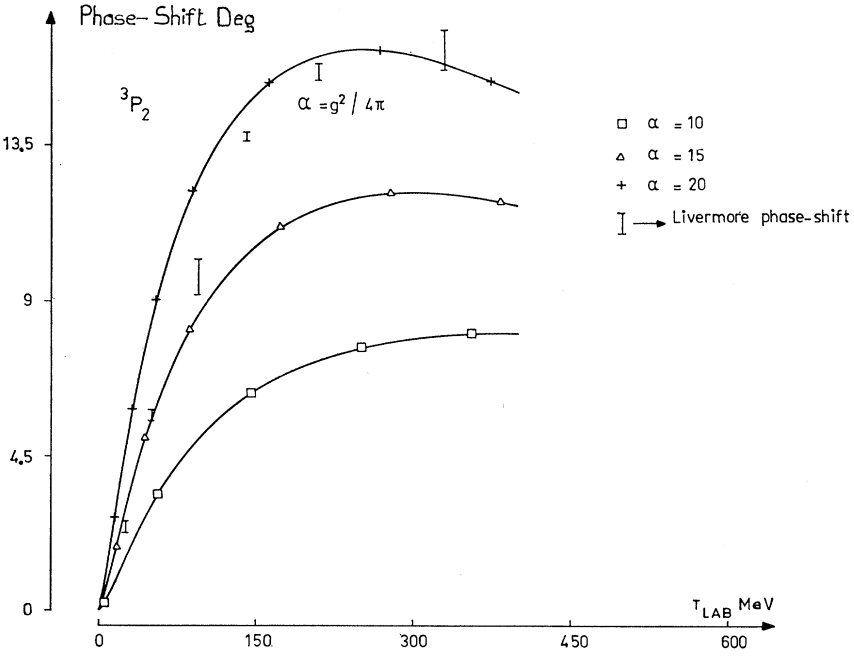


FIG. 22. Comparison between the experimental phase shifts and the Padé solution for three values of the coupling constant $\alpha = g^2/4\pi$, for the $^3P_2$ wave.

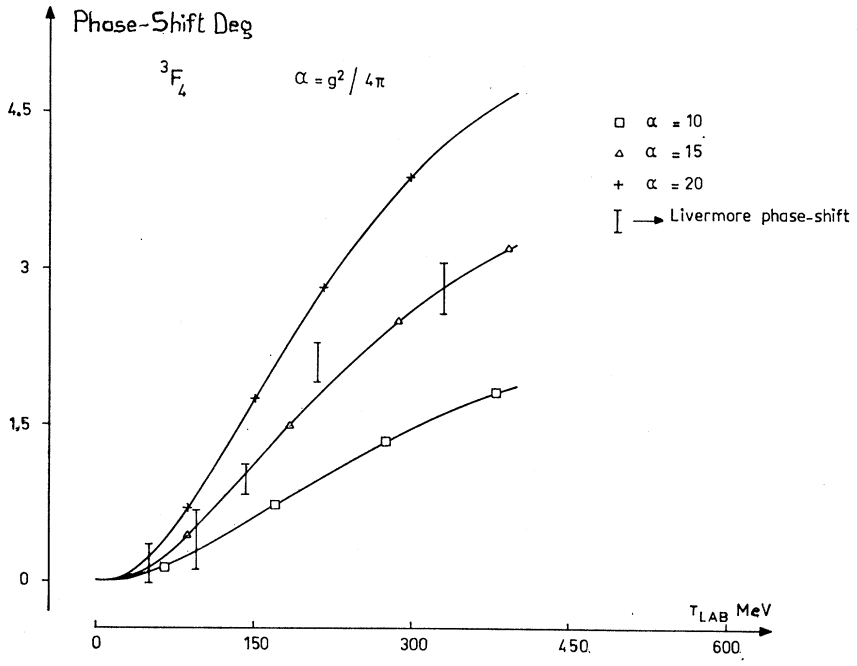


FIG. 23. Comparison between the experimental phase shifts and the Padé solution for three values of the coupling constant $\alpha = g^2/4\pi$, for the $^3F_4$ wave.

often gives wrong threshold behavior. It only gives rise to bound states in partial waves where they are present. However, it is highly inexact in reproducing other aspects, which are generally considered as due to other forces than pion exchange. For instance:

(1) The lower waves do not exhibit the change in sign generally attributed to the presence of repulsive cores;

(2) the $^1S_0$ wave is pathological because of the wrong threshold behavior of the Born term;

(3) the numerical values of the bound state and resonance energies are not obtained correctly with the physical value of the coupling constant $\alpha = 15$; also, the residues of the corresponding poles are badly represented.

These defects, which are unavoidable in such a low-order approximation, can be eliminated in two ways. Either one can compute higher perturbative orders, in order to build higher-order Padé approximants, or one can introduce other forces in the theory. In the former

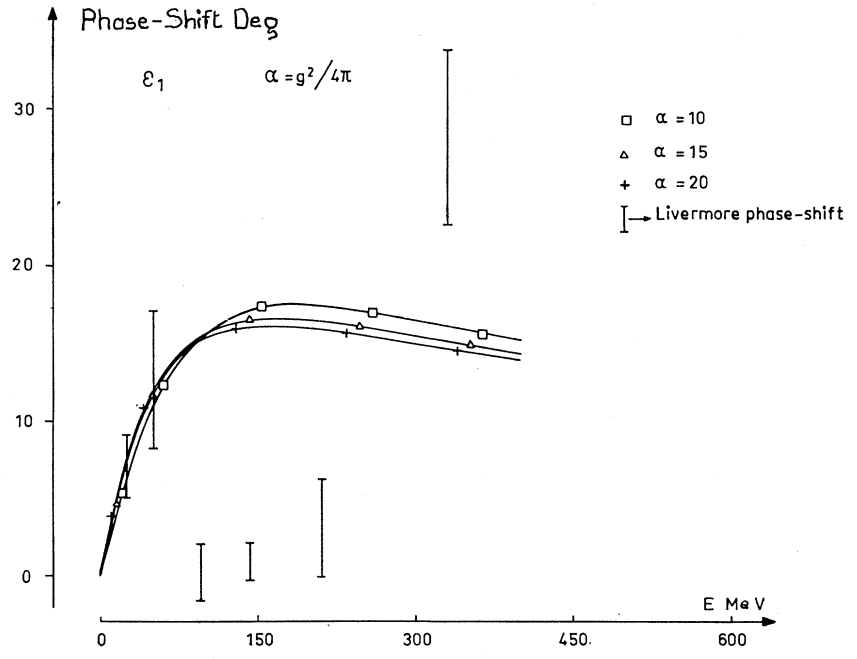


FIG. 24. Comparison between the experimental phase shifts and the Padé solution for three values of the coupling constant $\alpha = g^2/4\pi$, for the $\epsilon_1$ wave.

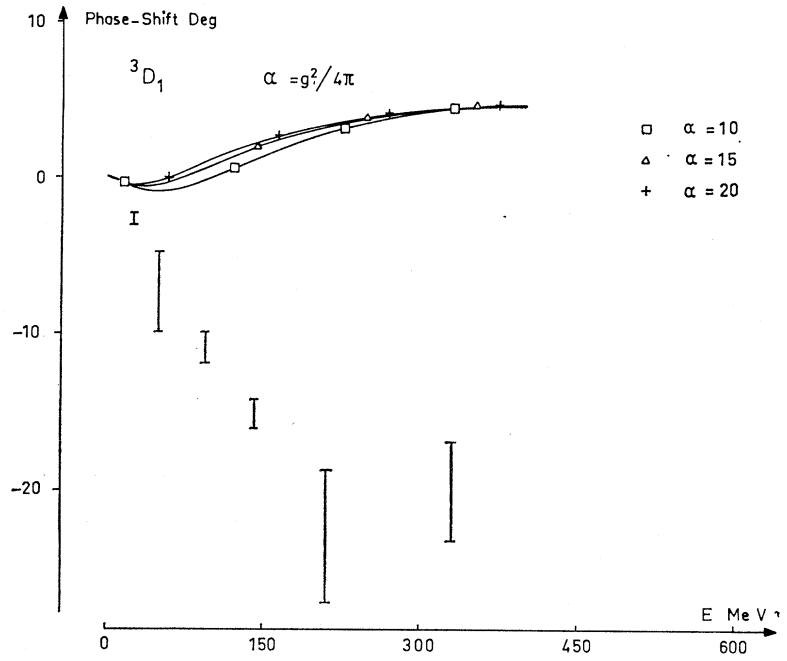


FIG. 25. Comparison between the experimental phase shifts and the Padé solution for three values of the coupling constant $\alpha=g^2/4\pi$, for the $^3D_1$ wave.

case, one has the direct continuation of the present method with pion exchange. In the latter case, one tries to insert more physical information in the Lagrangian, in order to describe phenomenologically the experimental situation with a low-order approximation. In view of the importance of the problem, our opinion is that both ways should be tried, with a preference for the first one, because it is necessary that convergence of the Padé method be achieved to get any sensible result. The forces due to the exchange of other pseudoscalar mesons can be treated in our theory, even at its present stage, by introducing the $K$, $\eta$, $\Lambda$, and $\Sigma$ fields within $SU(3)$ symmetry. It is obvious, however, that things will not change drastically by the introduction of the $K$ and $\eta$ mesons, which have the same spin-parity properties as the pion, and much larger masses. Also, since $SU(3)$ is not very well satisfied, one would be forced to introduce some extra arbitrary parameters. In any case, the computations of Wortman[21] show clearly that the modifications induced by the introduc-

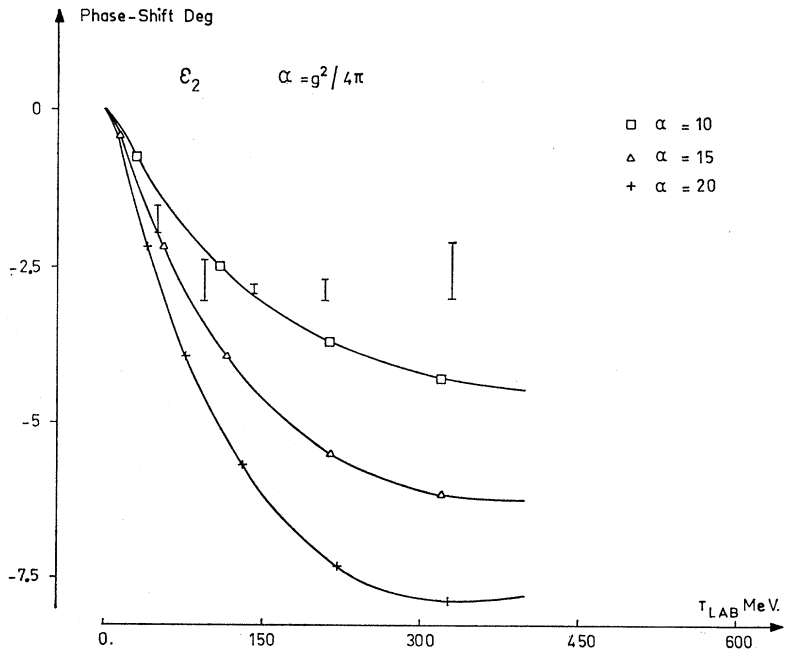


FIG. 26. Comparison between the experimental phase shifts and the Padé solution for three values of the coupling constant $\alpha=g^2/4\pi$, for the $\epsilon_2$ wave.

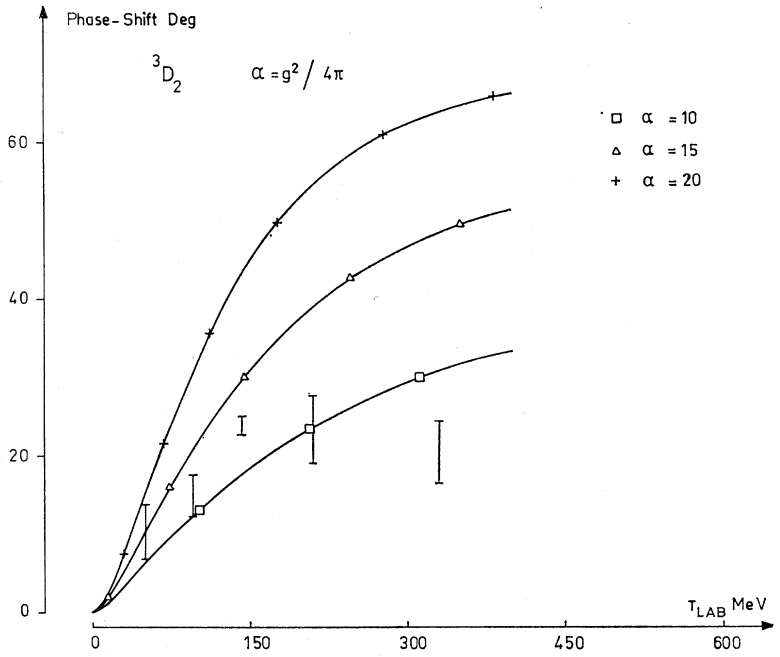


FIG. 27. Comparison between the experimental phase shifts and the Padé solution for three values of the coupling constant $\alpha = g^2/4\pi$, for the $^3D_2$ wave.

tion of the complete meson and baryon octets are small. However, these fields will naturally be considered when considering the $\Lambda N$, $\Sigma N$, etc., interactions. More interesting would be a computation of $N$-$N$ scattering based on the $\sigma$ model according to the recent results of Ref. 27 for the case of the mesons.

We conclude by saying that the model presented in this paper has some entirely new features compared to those used up to now in nucleon-nucleon scattering, and that these first encouraging results give hope for further improvements and developments.

## ACKNOWLEDGMENTS

We would like to thank Professor M. Froissart for his help and illuminating discussions throughout this work. Professor J. L. Basdevant, Professor R. Stora, and Professor J. Zinn-Justin are thanked for many discussions and for their interest. Three of us (S. G., V. G., G. T.) would like to thank Professor C. Bloch for his warm hospitality at the Saclay Theoretical Division.

## APPENDIX A: METHOD OF NUMERICAL CALCULATION OF FROISSART-GRIBOV INTEGRALS

We describe here a sophisticated method for computing the Froissart-Gribov integrals in the physical region.[29] With this method we have obtained a high accuracy such as $10^{-4}$ with few points (typically five points).

[29] We thank Dr. J. L. Basdevant for suggesting this method to us.

A typical Froissart-Gribov integral is

$$a_J^{(n)}(s) = \int_{t_0}^{\infty} A^{(n)}(s,t') Q_J\left(1+\frac{2t'}{s-4m^2}\right) dt', \quad \text{(A1)}$$

where $A^{(n)}(s,t')$ is the absorptive part in the $t$ channel of the $n$th-order term of the renormalized perturbative amplitude. We want to exploit the fact that $A^{(n)}(s,t')$ *is analytic by pieces* in the variable $t'$. If $A^{(n)}(s,t')$ has singularities for $t' > t_0$, one has to cut the integral into a certain number of parts such that the singularities fall at the end points of the integration path. Then by a suitable change of variables one can always get rid of one singularity by mapping the corresponding point with infinity; in this way one is back to the previous conditions, but now with $A^{(n)}(s,t')$ analytic in $t'$.

In general, $A^{(n)}(s,t')$ will have a square-root singularity at $t' = t_0$, which necessitates a particular method of integration. At $t' = \infty$, $A^{(n)}(s,t')$ will behave like $(\ln t')^n$.

If we perform the change of variable

$$t' = t_0 \cosh^2(x/2J), \quad \text{(A2)}$$

then

$$a_J^{(n)}(s) = \int_0^{\infty} f_J^{(n)}(s,x) e^{-x} dx, \quad \text{(A3)}$$

with

$$f_J^{(n)}(s,x) = \left\{\frac{t_0}{2J} e^x \sinh\frac{x}{J} Q_J\left[1+\frac{2t_0}{s-4m^2}\cosh^2\left(\frac{x}{2J}\right)\right]\right\} \times A^{(n)}\left[s, t_0 \cosh^2\left(\frac{x}{2J}\right)\right],$$

where now two conditions for $f_J^{(n)}(s,x)$ are fulfilled: (1) $f_J^{(n)}(s,x)\sim x^n$ when $x\to\infty$, and (2) $f_J^{(n)}(s,x)$ is analytic in a neighborhood of the integration path. There exists a parabola with focus at the origin in the $x$ plane and whose axis is the real positive axis, and inside this parabola $f_J^{(n)}(s,x)$ is analytic.

The "kinematical" factor

$$\frac{t_0}{2J}e^x \sinh\frac{x}{J} Q_J\left[1+\frac{2t_0}{s-4m^2}\cosh^2\left(\frac{x}{2J}\right)\right] \quad \text{(A4)}$$

has singularities in the $x$ plane for

$$x=\pm iJ\pi,\ \pm 3iJ\pi,\ \ldots \quad \text{(A5)}$$

and

$$\cos\frac{ix}{2J}=\pm\left(\frac{4m^2-s}{t_0}\right)^{1/2}. \quad \text{(A6)}$$

We notice that for the parabola to exist, it is necessary that Eq. (A6) has no solution with $x$ real and positive. Such solutions occur only when $s$ is real and smaller than $4m^2-t_0$. In particular, in the physical region where $s\geq 4m^2$, the parabola always exists since the only singularity of $A^{(n)}(s,t')$ on the integration path is assumed to be at $t_0$. This singularity is removed in the transformation (A2).

We now use the Gauss-Laguerre method of integration. We replace

$$a_J^{(n)}(s)=\int_0^\infty f_J^{(n)}(s,x)e^{-x}dx$$

by

$$\bar{a}_J^{(n)}(s)=\sum_{i=1}^{N} f_J^{(n)}(s,x_i)\omega_i, \quad \text{(A7)}$$

where the $x_i$ are the zeros of the Laguerre polynomials and $\omega_i$ are the corresponding weights.[30] We expect that the difference between (A3) and (A7) is of order $e^{-N\Delta}$, where $\Delta$ is the distance between the focus and the top of the parabola. We see here the importance of trying to get the largest possible parabola. In particular, when the parabola flattens down (for instance, for $s<4m^2-t_0$), then we lose the exponential convergence and come back to the usual convergence.

Obviously, one can always construct the set of orthogonal polynomials with respect to a measure having the prescribed type of end-point singularities. However, in practice this may be a complication, except when one has to deal very often with definite types of singularities. Anyhow, the idea is always to try to get the maximal analyticity domain around the path of integration in such a way as to obtain exponential convergence.

[30] The values of the zeros and their corresponding weights can be found in Z. Kopal, *Numerical Analysis* (Chapman, London, 1961), Appendix IV.2.

## APPENDIX B

### 1. Notation and Definitions

Our metric will be defined by the metric tensor

$$g_{00}=1,\quad g_{\mu\nu}=-1 \quad \text{for} \quad \mu=\nu=1,2,3,$$
$$g_{\mu\nu}=0,\quad \mu\neq\nu. \quad \text{(B1)}$$

The scalar product is then

$$a\cdot b=a_0b_0-\mathbf{a}\cdot\mathbf{b}. \quad \text{(B2)}$$

The Dirac equations for the spinors $u(p,s)$ and $v(p,s)$ read

$$\begin{aligned}(\gamma\cdot p-m)u(p,s)&=0,\\ (\gamma\cdot p+m)v(p,s)&=0,\end{aligned} \quad \text{(B3)}$$

where we have defined

$$\gamma\cdot p=p_0\gamma_0-\mathbf{p}\cdot\boldsymbol{\gamma}.$$

We normalize the spinors in such a way that

$$\bar{u}u=-\bar{v}v=1,\quad \text{where}\quad \bar{u}=u^\dagger\gamma_0.$$

For the Dirac matrices we use the representation in which $\gamma_0$ is diagonal and $\gamma_5$ is antidiagonal; i.e.,

$$\gamma_0=\begin{bmatrix}1 & 0\\ 0 & -1\end{bmatrix},\quad \boldsymbol{\gamma}=\begin{bmatrix}0 & \boldsymbol{\sigma}\\ -\boldsymbol{\sigma} & 0\end{bmatrix},\quad \gamma_5=\begin{bmatrix}0 & 1\\ 1 & 0\end{bmatrix}, \quad \text{(B4)}$$

where

$$\gamma_5=i\gamma_0\gamma_1\gamma_2\gamma_3. \quad \text{(B5)}$$

The $\sigma_i$ are the $2\times 2$ Pauli matrices. In this representation one has

$$(\gamma_5)^2=(\gamma_0)^2=-(\boldsymbol{\gamma})^2=1. \quad \text{(B6)}$$

For completeness, we quote also the well-known anticommutation relations of the $\gamma$ matrices:

$$[\gamma_\mu,\gamma_\nu]_+=2g_{\mu\nu}. \quad \text{(B7)}$$

The tensor operator is defined in the usual way:

$$\sigma_{\mu\nu}=\tfrac{1}{2}i[\gamma_\mu,\gamma_\nu].$$

### 2. Kinematics

We label by $p_1$, $p_2$ and $p_1'$, $p_2'$ the four-momenta of the ingoing and outgoing nucleons, respectively. We define the Mandelstam variables $s$, $t$, and $u$, as usual, by

$$\begin{aligned}s&=(p_1+p_2)^2=(p_1'+p_2')^2,\\ t&=(p_1-p_1')^2=(p_2-p_2')^2,\\ u&=(p_2-p_1')^2=(p_1-p_2')^2,\end{aligned} \quad \text{(B8)}$$

so that we have

$$s+t+u=4m^2,$$

where $m$ is the nucleon mass. Since nucleon-nucleon kinematics is well known, we will not be discussing it here.

The following linear combinations of the four-vectors $p_i$, $p_i'$ will be useful:

$$\begin{aligned}\Pi_1&=\tfrac{1}{2}(p_1+p_1'),\\ \Pi_2&=\tfrac{1}{2}(p_2+p_2'),\\ \Pi&=\tfrac{1}{2}(p_1+p_2)=\tfrac{1}{2}(p_1'+p_2').\end{aligned}\tag{B9}$$

We quote also the well-known kinematical relations

$$s=4(p^2+m^2)=4E^2,\tag{B10}$$

$$t=-2p^2(1-\cos\theta_s),\tag{B11}$$

$$u=-2p^2(1+\cos\theta_s),\tag{B12}$$

where $p$ is the c.m. momentum of each nucleon, $E$ is the c.m. energy of each nucleon, and $\theta_s$ is the c.m. scattering angle in the $s$ channel. Let us recall also that in this picture the $s$ channel describes a nucleon-nucleon process, whereas the $t$ and $u$ channels describe nucleon-antinucleon processes.

### 3. Useful Definitions and Relations Involving Fermi Invariants

The decomposition of the nucleon-nucleon amplitude on invariant spinor amplitudes, is a classical problem, and it is particularly well discussed in Ref. 5. We only recall here the definitions and the most useful relations.

A well suited set of invariants is the classical Fermi set, which is defined in the following way:

$$\begin{aligned}S&=\bar u(p_1')u(p_1)\bar u(p_2')u(p_2),\\ V&=\bar u(p_1')\gamma_{(1)}{}^{\mu}u(p_1)\bar u(p_2')\gamma_{\mu}{}^{(2)}u(p_2),\\ T&=\tfrac{1}{2}\bar u(p_1')\sigma_{(1)}{}^{\mu\nu}u(p_1)\bar u(p_2')\sigma_{\mu\nu}{}^{(2)}u(p_2),\\ A&=\bar u(p_1')i\gamma_{(1)}{}^{5}\gamma_{(1)}{}^{\mu}u(p_1)\bar u(p_2')i\gamma_5{}^{(2)}\gamma_{\mu}{}^{(2)}u(p_2),\\ P&=\bar u(p_1')\gamma_{(1)}{}^{5}u(p_1)\bar u(p_2')\gamma_5{}^{(2)}u(p_2).\end{aligned}\tag{B13}$$

The invariants $\tilde S$, $\tilde V$, $\tilde T$, $\tilde A$, $\tilde P$ can be obtained from $S$, $V$, $T$, $A$, $P$ by interchanging the final particles, i.e., with the interchange

$$p_2'\leftrightarrow p_1'.$$

By the same interchange, we have also

$$s\leftrightarrow s,\quad t\leftrightarrow u.$$

Between the two sets there is a linear relation, which reads

$$\begin{pmatrix}\tilde S\\ \tilde V\\ \tilde T\\ \tilde A\\ \tilde P\end{pmatrix}=\tfrac{1}{4}\begin{pmatrix}1&1&1&1&1\\ 4&-2&0&2&-4\\ 6&0&-2&0&6\\ 4&2&0&-2&-4\\ 1&-1&1&-1&1\end{pmatrix}\begin{pmatrix}S\\ V\\ T\\ A\\ P\end{pmatrix}.\tag{B14}$$

We quote also the following relation, whose usefulness can be recognized in the antisymmetrization of the perturbative diagrams:

$$\begin{pmatrix}S+\tilde S\\ T-\tilde T\\ A+\tilde A\\ V-\tilde V\\ P+\tilde P\end{pmatrix}=\tfrac{1}{2}\begin{pmatrix}0&1&0&1&0\\ -6&0&0&0&-6\\ 0&0&0&2&0\\ -4&0&-2&0&4\\ 0&1&0&-1&0\end{pmatrix}\begin{pmatrix}S-\tilde S\\ T+\tilde T\\ A-\tilde A\\ V+\tilde V\\ P-\tilde P\end{pmatrix}.\tag{B15}$$

Another well-suited set of invariants is defined by Amati, Leader, and Vitale[5]; it is called the set of "perturbative invariants." In our notation and metric they are defined by the following formulas:

$$\begin{aligned}P_1&=S,\\ P_2&=-[\bar u(p_1')u(p_1)\bar u(p_2')\gamma\cdot\Pi_1u(p_2)\\ &\qquad+\bar u(p_1')\gamma\cdot\Pi_2u(p_1)\bar u(p_2')u(p_2)],\\ P_3&=\bar u(p_1')\gamma\cdot\Pi_2u(p_1)\bar u(p_2')\gamma\cdot\Pi_1(p_2),\\ P_4&=V,\\ P_5&=P.\end{aligned}\tag{B16}$$

The relation between the perturbative basis and the Fermi basis is given in Ref. 5, and reads

$$\begin{aligned}P_2&=[(u-s)S-4m^2V+tT+(u-s)P]/4m,\\ P_3&=\tfrac{1}{4}[-(u-s)V-tA+4m^2P].\end{aligned}\tag{B17}$$

We also define the following quantities, which are found useful in the computations:

$$\begin{aligned}(IP)_2&=\bar u(p_1')\gamma\cdot\Pi u(p_1)\bar u(p_2')u(p_2)\\ &\qquad+\bar u(p_1')u(p_1)\bar u(p_2')\gamma\cdot\Pi u(p_2),\\ (IP)_3&=\bar u(p_1')\gamma\cdot\Pi u(p_1)\bar u(p_2')\gamma\cdot\Pi u(p_2).\end{aligned}\tag{B18}$$

The simple formulas which connect these invariants with the usual ones are

$$\begin{aligned}(IP_2)&=\tfrac{1}{2}(2mS-P_2)=-[(u-s-8m^2)S-4m^2V+tT\\ &\qquad+(u-s)P]/8m,\\ (IP)_3&=\tfrac{1}{4}(m^2S-mP_2+P_3)\\ &=\tfrac{1}{16}[(2s+t)(S+V+P)-t(T+A)].\end{aligned}\tag{B19}$$

### 4. Isospin Notation

We follow the standard notation: The charge spinors will be indicated by $\chi$ and $\chi^\dagger$, and the nucleon isotopic-spin operator by $\boldsymbol{\tau}$, where

$$\tau_j{}^2=1.$$

The projection operators on the states $T=0$ and $T=1$, are represented, respectively, by $\mathcal{P}_0$ and $\mathcal{P}_1$. They are expressed by the formulas

$$\begin{aligned}\mathcal{P}_0&=\tfrac{1}{4}(1-\boldsymbol{\tau}_1\cdot\boldsymbol{\tau}_2),\\ \mathcal{P}_1&=\tfrac{1}{4}(3+\boldsymbol{\tau}_1\cdot\boldsymbol{\tau}_2).\end{aligned}\tag{B20}$$

## APPENDIX C

### 1. Perturbative Diagrams

The most general $N$-$N$ scattering amplitude can be written as

$$\mathcal{T}=[F_1^0(S-\tilde{S})+F_2^0(T+\tilde{T})+F_3^0(A-\tilde{A})+F_4^0(V+\tilde{V})+F_5^0(P-\tilde{P})]\mathcal{P}_0+[F_1^1(S-\tilde{S})+F_2^1(T+\tilde{T})+F_3^1(A-\tilde{A})+F_4^1(V+\tilde{V})+F_5^1(P-\tilde{P})]\mathcal{P}_1. \quad \text{(C1)}$$

The interest in writing the amplitude in the form C1 is that the Pauli principle is then expressed by the simple relation

$$F_i^I(s,t,u)=(-)^{i+I}F_i^I(s,u,t). \quad \text{(C2)}$$

Instead of using the amplitudes $F_i^I$, it will be more convenient to use the following linear combinations:

$$\begin{aligned} G_1&=(1/4\pi)(F_1-4F_3+F_5),\\ G_2&=(1/2\pi)F_2,\\ G_3&=(1/4\pi)(F_1-2F_3-F_5),\\ G_4&=(1/2\pi)F_4,\\ G_5&=(1/4\pi)(F_1+4F_3+F_5). \end{aligned} \quad \text{(C3)}$$

In this appendix, we shall give the complete and explicit computation of the perturbative diagrams up to fourth order. For each graph we give the ten scalar amplitudes $G_i^T(s,t,u)$ and then in terms of these $G_i^T$ we give the contribution to the partial waves, using the formulas (4.25) of GGMW, which read

$$f_0^J(s)=\frac{P}{2E}\int_{-1}^{1}f_1(s,z)P_J(z)dz \quad \text{(C4)}$$

for the singlet,

$$\begin{aligned} f_{11}^J(s)&=\frac{P}{2E}\int_{-1}^{1}f_2(s,z)P_J(z)dz,\\ f_{12}^J(s)&=\frac{P}{2m}\int_{-1}^{1}f_5(s,z)\frac{[J(J+1)]^{1/2}}{2J+1}\times[P_{J+1}(z)-P_{J-1}(z)]dz, \quad \text{(C5)}\\ f_{22}^J(s)&=\frac{P}{2E}\int_{-1}^{1}\left[f_3(s,z)P_J(z)+\frac{JP_{J+1}(z)+(J+1)P_{J-1}(z)}{2J+1}f_4(s,z)\right]dz \end{aligned}$$

for the coupled triplet, and

$$f_1^J(s)=\frac{P}{2E}\int_{-1}^{1}\left[f_4(s,z)P_J(z)+\frac{JP_{J+1}(z)+(J+1)P_{J-1}(z)}{2J+1}f_3(s,z)\right]dz \quad \text{(C6)}$$

for the uncoupled triplet, where

$$z=\cos\theta_s,$$

and

$$\begin{aligned} f_1&=E^2G_1-zp^2G_2+m^2G_3,\\ f_2&=(E^2G_2+m^2G_4)z-p^2G_5,\\ f_3&=-p^2G_3,\\ f_4&=m^2G_2+E^2G_4,\\ f_5&=-m^2(G_2+G_4). \end{aligned} \quad \text{(C7)}$$

We define

$$G_i^{J,T}(s)=\int_{-1}^{1}G_i^T(s,z)P_J(z)dz. \quad \text{(C8)}$$

The partial-wave amplitudes can be rewritten in the following way:

$$\begin{aligned} f_0^J&=\frac{1}{8}\left(\frac{s-4m^2}{s}\right)^{1/2}\left[sG_1^J+4m^2G_3^J-\frac{J+1}{2J+1}(s-4m^2)\times G_2^{J+1}-\frac{J}{2J+1}(s-4m^2)G_2^{J-1}\right],\\ f_{11}^J&=\frac{1}{8}\left(\frac{s-4m^2}{s}\right)^{1/2}\left[s\frac{J+1}{2J+1}G_2^{J+1}+\frac{J}{2J+1}sG_2^{J-1}+4m^2\frac{J+1}{2J+1}G_4^{J+1}+4m^2\frac{J}{2J+1}\times G_4^{J-1}-(s-4m^2)G_5^J\right],\\ f_{12}^J&=-\tfrac{1}{4}m(s-4m^2)^{1/2}\frac{[J(J+1)]^{1/2}}{2J+1}\times(G_2^{J+1}-G_2^{J-1}+G_4^{J+1}-G_4^{J-1}),\\ f_{22}^J&=\frac{1}{8}\left(\frac{s-4m^2}{s}\right)^{1/2}\left[-(s-4m^2)G_3^J+\frac{J}{2J+1}4m^2G_2^{J+1}+\frac{J+1}{2J+1}4m^2G_2^{J-1}+\frac{J}{2J+1}sG_4^{J+1}+\frac{J+1}{2J+1}sG_4^{J-1}\right],\\ f_1^J&=\frac{1}{8}\left(\frac{s-4m^2}{s}\right)^{1/2}\left[4m^2G_2^J+sG_4^J-(s-4m^2)\times\frac{J}{2J+1}G_3^{J+1}-(s-4m^2)\frac{J+1}{2J+1}G_3^{J-1}\right]. \end{aligned} \quad \text{(C9)}$$

We next transform Eq. (C8) by means of the Froissart-Gribov formula. The expression for the $G_i^{J,T}(s)$

is then

$$G_i^{J,T}(s)=\frac{8}{\pi(s-4m^2)}\int_{t_0}^{\infty}\mathrm{Abs}_t G_i^T(s,t')\times Q_J\left(1+\frac{2t'}{s-4m^2}\right)dt'. \quad \text{(C10)}$$

(In this equation the Pauli principle has been taken into account.) It is therefore sufficient to compute the absorptive parts of $G_i^T$ in the $t$ channel in order to obtain the partial-wave projections of the fourth-order diagrams. In Eq. (C10), $t_0$ will be $4m^2$ for the vertex and self-energy graphs, and $4\mu^2$ for the direct and crossed two-pion-exchange graphs. Another important feature of the formula (C10) is that it gives automatically the correct analytic continuation in complex $J$ plane, as is well known.

### 2. Connection between Phase Shifts and Amplitudes in Nucleon-Nucleon System

In the notation of GGMW, we define the partial-wave amplitude in terms of the usual nuclear-bar phase shifts.[18] For the singlet amplitude, we have

$$f_0^J=(e^{2i\delta_{0J}}-1)/i\,; \quad \text{(C11)}$$

for the uncoupled triplet,

$$f_1^J=(e^{2i\delta_{1J}}-1)/i\,; \quad \text{(C12)}$$

and for the coupled triplet,

$$\begin{aligned} f_{l=J-1}&=[\cos 2\bar{\epsilon}_J\exp(2i\bar{\delta}_{l=J-1})-1]/i,\\ f_{l=J+1}&=[\cos 2\bar{\epsilon}_J\exp(2i\bar{\delta}_{l=J+1})-1]/i. \quad \text{(C13)}\\ f_{J-1,J+1}&=\sin 2\epsilon_J\exp[i(\bar{\delta}_{l=J-1}+\bar{\delta}_{l=J+1})]. \end{aligned}$$

Defining the amplitude for the coupled triplet by

$$f=\begin{pmatrix} f_{l=J-1} & f_{J-1,J+1}\\ f_{J-1,J+1} & f_{l=J+1}\end{pmatrix}, \quad \text{(C14)}$$

the elastic unitarity condition reads

$$2\,\mathrm{Im}f=ff^*. \quad \text{(C15)}$$

(Notice that our amplitudes are identical to those of Ball, Scotti, and Wong[19] up to a multiplicative factor $E/2mp$.) The amplitudes (C13) are deduced from the amplitudes $f_{11}^J$, $f_{12}^J$, and $f_{22}^J$, defined in GGMW, by means of the linear transformation (D6).

### 3. Computation of Born Term

The results of this computation, given here essentially for completeness, are obviously identical to those of GGMW. The contribution of the Born term to the $G_i^T$ amplitudes is

$$\begin{aligned} G_1^0&=-G_3^0=G_5^0=\frac{3}{8\pi}g^2\left(\frac{1}{u-\mu^2}-\frac{1}{t-\mu^2}\right),\\ G_2^0&=-G_4^0=-\frac{3}{8\pi}g^2\left(\frac{1}{u-\mu^2}+\frac{1}{t-\mu^2}\right),\\ G_1^1&=-G_3^1=G_5^1=\frac{1}{8\pi}g^2\left(\frac{1}{u-\mu^2}+\frac{1}{t-\mu^2}\right),\\ G_2^1&=-G_4^1=-\frac{1}{8\pi}g^2\left(\frac{1}{u-\mu^2}-\frac{1}{t-\mu^2}\right), \end{aligned}$$

where $g$ is the renormalized pion-nucleon coupling constant, and $\mu$ is the pion mass. The partial-wave projections of this Born term are given in Appendix D1.

### 4. Self-Energy and Vertex Diagrams

The corresponding Feynman diagrams are shown in Fig. 28. We define the following functions:

$$\Pi(t)=\frac{1}{2}\int_{4m^2}^{\infty}\frac{dt'}{t'-t}\frac{t'}{(t'-\mu^2)^2}\left(\frac{t'-4m^2}{t'}\right)^{1/2} \quad \text{(C16)}$$

for Fig. 28(a), and

$$V(t)=\int_{4m^2}^{\infty}\frac{dt'}{t'-t}\frac{1}{t'-\mu^2}\left[\left(\frac{t'-4m^2}{t'}\right)^{1/2}-\mu^2\frac{\ln[1+(t'-4m^2)/\mu^2]}{[t'(t'-4m^2)]^{1/2}}\right] \quad \text{(C17)}$$

for Fig. 28(b) and the one having the pion correction on the lower vertex whose contributions are identical. The sum of previous graphs gives

$$H(t)=-\frac{g^4}{2\pi^2}\Pi(t)+\frac{g^4}{8\pi^2}V(t), \quad \text{(C18)}$$

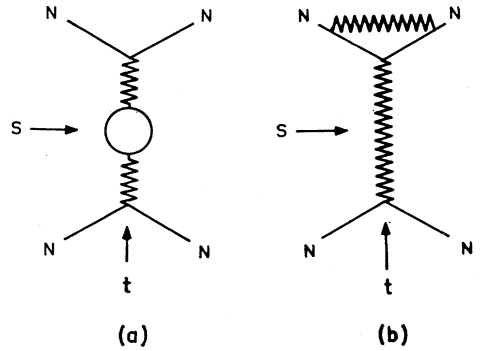


FIG. 28. (a) Self-energy diagram in the $N$-$N$ elastic amplitude. (b) Vertex diagram in the $N$-$N$ elastic amplitude.

and the $G_i^T$ amplitudes read

$$\begin{aligned} G_1^0 &= -G_3^0 = G_5^0 = (3/8\pi)[H(u)-H(t)], \\ G_2^0 &= -G_4^0 = -(3/8\pi)[H(u)+H(t)], \\ G_1^1 &= -G_3^1 = G_5^1 = (1/8\pi)[H(u)+H(t)], \\ G_2^1 &= -G_4^1 = -(1/8\pi)[H(u)-H(t)]. \end{aligned} \tag{C19}$$

It is then straightforward to project out the partial-wave amplitudes. Defining $\rho(t)$ as

$$\rho(t) = -(8\pi/g^4)\,\mathrm{Im}_t H(t)(t-\mu^2) \tag{C20}$$

$$= \frac{t+\mu^2}{t-\mu^2}\left(\frac{t-4m^2}{t}\right)^{1/2} + \mu^2 \frac{\ln[1+(t-4m^2)/\mu^2]}{[t(t-4m^2)]^{1/2}}, \tag{C21}$$

and introducing

$$A^J(s) = \int_{4m^2}^{\infty} \frac{dt'}{t'-\mu^2}\rho(t')Q_J\left(1+\frac{2t'}{s-4m^2}\right), \tag{C22}$$

we obtain

$$\begin{aligned} f_0^{J,0} &= \frac{3}{4\pi}\alpha^2\gamma\left(A^J - \frac{J+1}{2J+1}A^{J+1} - \frac{J}{2J+1}A^{J-1}\right), \\ f_0^{J,1} &= -\tfrac{1}{3}f_0^{J,0}, \\ f_{11}^{J,0} &= -f_0^{J,0}, \quad f_{11}^{J,1} = -\tfrac{1}{3}f_{11}^{J,0} = -f_0^{J,1}, \\ f_{22}^{J,0} &= \frac{3}{4\pi}\alpha^2\gamma\left(A^J - \frac{J}{2J+1}A^{J+1} - \frac{J+1}{2J+1}A^{J-1}\right), \\ f_{22}^{J,1} &= -\tfrac{1}{3}f_{22}^{J,0}, \\ f_1^{J,0} &= -f_{22}^{J,0}, \quad f_1^{J,1} = -\tfrac{1}{3}f_1^{J,0} = -f_{22}^{J,1}, \\ f_{12}^{J,T} &\equiv 0, \\ f_0^{0,1} &= -f_{11}^{0,1} = (1/4\pi)\alpha^2\gamma(A^1 - A^0), \end{aligned} \tag{C23}$$

where $\alpha = g^2/4\pi$ and $\gamma = [(s-4m^2)/s]^{1/2}$.

### 5. Box Diagram

The Feynman diagram to be computed now is represented in Fig. 29. Let us define

$$\begin{aligned} B(s,t;m^2,\mu^2) &= \int_0^1 [\delta(1-\sum_{i=1}^4 z_i)\prod_{i=1}^4 dz_i]/[-z_1z_2s - z_3z_4t \\ &\quad + m^2(z_1+z_2)^2 + \mu^2(z_3+z_4)], \\ B_1(s,t) &= \frac{\partial}{\partial m^2}B(s,t), \\ B_2(s,t) &= B_1(s,t) + 4\frac{\partial}{\partial s}B(s,t), \end{aligned} \tag{C24}$$

where the $z_i$ are the Feynman parameters. The contributions to the $G_i^T$ amplitudes are then

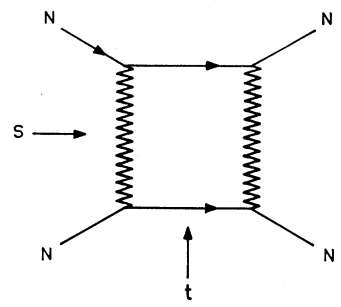


FIG. 29. Box diagram in the $N$-$N$ elastic amplitude.

$$\begin{aligned} G_1^0 &= -(3\alpha^2/32\pi)\{-3(4m^2-s)[B_1(s,t)-B_1(s,u)] \\ &\quad -9s[B_2(s,t)-B_2(s,u)] - 12[tB_2(s,t)-uB_2(s,u)] \\ &\quad -24[B(s,t)-B(s,u)]\}, \end{aligned} \tag{C25}$$

$$\begin{aligned} G_1^1 &= -(\alpha^2/32\pi)\{-(4m^2-s)[B_1(s,t)+B_1(s,u)] \\ &\quad -3s[B_2(s,t)+B_2(s,u)] - 4[tB_2(s,t)+uB_2(s,u)] \\ &\quad -8[B(s,t)+B(s,u)]\}, \end{aligned} \tag{C26}$$

$$\begin{aligned} G_2^0 &= -(3\alpha^2/32\pi)\{3(4m^2-s)[B_1(s,t)+B_1(s,u)] \\ &\quad -3s[B_2(s,t)+B_2(s,u)]\}, \end{aligned} \tag{C27}$$

$$\begin{aligned} G_2^1 &= -(\alpha^2/32\pi)\{(4m^2-s)[B_1(s,t)-B_1(s,u)] \\ &\quad -s[B_2(s,t)-B_2(s,u)]\}, \end{aligned} \tag{C28}$$

$$\begin{aligned} G_3^0 &= -(3\alpha^2/32\pi)\{3(4m^2-s)[B_1(s,t) \\ &\quad -B_1(s,u)] + 3s[B_2(s,t)-B_2(s,u)] \\ &\quad +12[B(s,t)-B(s,u)]\}, \end{aligned} \tag{C29}$$

$$\begin{aligned} G_3^1 &= -(\alpha^2/32\pi)\{(4m^2-s)[B_1(s,t)+B_1(s,u)] \\ &\quad +s[B_2(s,t)+B_2(s,u)] \\ &\quad +4[B(s,t)+B(s,u)]\}, \end{aligned} \tag{C30}$$

$$\begin{aligned} G_4^0 &= -(3\alpha^2/32\pi)\{-3(4m^2-s)[B_1(s,t)+B_1(s,u)] \\ &\quad -3s[B_2(s,t)+B_2(s,u)] \\ &\quad -12[B(s,t)+B(s,u)]\}, \end{aligned} \tag{C31}$$

$$\begin{aligned} G_4^1 &= -(\alpha^2/32\pi)\{-(4m^2-s)[B_1(s,t)-B_1(s,u)] \\ &\quad -s[B_2(s,t)-B_2(s,u)] \\ &\quad -4[B(s,t)-B(s,u)]\}, \end{aligned} \tag{C32}$$

$$\begin{aligned} G_5^0 &= -(3\alpha^2/32\pi)\{9(4m^2-s)[B_1(s,t)-B_1(s,u)] \\ &\quad -12[tB_1(s,t)-uB_1(s,u)] + 3s[B_2(s,t)-B_2(s,u)] \\ &\quad +24[B(s,t)-B(s,u)]\}, \end{aligned} \tag{C33}$$

$$\begin{aligned} G_5^1 &= -(\alpha^2/32\pi)\{3(4m^2-s)[B_1(s,t)+B_1(s,u)] \\ &\quad -4[tB_1(s,t)+uB_1(s,u)] + s[B_2(s,t)+B_2(s,u)] \\ &\quad +8[B(s,t)+B(s,u)]\}. \end{aligned} \tag{C34}$$

In order to project out the partial-wave amplitudes, we need to know the absorptive parts $\mathrm{Abs}_t G_i^T$ in the $t$ channel of the $G_i^T$ amplitudes, i.e., the absorptive parts of the $B$ functions. These quantities can be computed

explicitly, and are given by the following formulas:

$$\mathrm{Im}_t B(s,t)=\frac{2\pi}{t^{1/2}}\frac{1}{s+t-4m^2}[\varphi(t)+\Psi(s,t)], \quad \text{(C35)}$$

where, if we define $\Delta=(s-4m^2)(t-4\mu^2)-4\mu^4$, the function $\varphi$ is given by

$$\varphi(t)=\frac{t-2\mu^2}{(t-4m^2)^{1/2}}Q_0\left(\frac{t-2\mu^2}{[(t-4m^2)(t-4\mu^2)]^{1/2}}\right). \quad \text{(C36)}$$

This function being defined in the region $t>4m^2$ can be analytically extended to the region $4\mu^2<t<4m^2$ where it is still real. In fact, it is enough to notice that we have, for $x<0$,

$$x^{-1/2}Q_0(x^{-1/2})=(-x)^{-1/2}\arctan(-x)^{1/2}.$$

The function $\Psi$ exhibits a discontinuity in $s$ that is just the same as that of the double spectral function of the Mandelstam representation:

$$\Psi(s,t)=\frac{\Delta^{1/2}}{s^{1/2}}\left[-Q_0\left(\frac{s^{1/2}(t-4\mu^2)^{1/2}}{\Delta^{1/2}}\right)+\tfrac{1}{2}i\pi\right] \quad \text{(C37)}$$

for $\Delta>0$, i.e., for $s>4m^2+4\mu^4/(t-4\mu^2)$ with $t>4\mu^2$. It is then easy to continue it analytically in the regions $\Delta<0$, $s>0$, $t>4\mu^2$:

$$\Psi(s,t)=-\frac{(-\Delta)^{1/2}}{s^{1/2}}\arctan\left(\frac{s(t-4\mu^2)}{-\Delta}\right)^{1/2}, \quad \text{(C38)}$$

for $\Delta<0$, $s<0$, $t>4\mu^2$:

$$\Psi(s,t)=-\frac{(-\Delta)^{1/2}}{(-s)^{1/2}}Q_0\left(\frac{-\Delta}{-s(t-4\mu^2)}\right)^{1/2}. \quad \text{(C39)}$$

For the $t$-channel absorptive parts of functions $B_1$ and $B_2$, the same relations hold as for the functions themselves; namely, we have

$$\begin{aligned}\mathrm{Im}_t B_1(s,t)&=\frac{\partial}{\partial m^2}\mathrm{Im}_t B(s,t;m^2,\mu^2),\\ \mathrm{Im}_t B_2(s,t)&=\frac{\partial}{\partial m^2}\mathrm{Im}_t B(s,t;m^2,\mu^2)\\ &\quad+4\frac{\partial}{\partial s}\mathrm{Im}_t B(s,t;m^2,\mu^2).\end{aligned} \quad \text{(C40)}$$

Taking into account these relations, it is easy to check that the double spectral function for $(G_2+G_4)^T$ vanishes and that its simple spectral function is given by

$$\bar\rho(t)=\frac{1}{\alpha^2}\mathrm{Im}_t(G_2+G_4)_{T=1}=\frac{1}{4}\left(\frac{t-4\mu^2}{t}\right)^{1/2}\times\frac{1}{t-4m^2}Q_1\left(\frac{t-2\mu^2}{[(t-4\mu^2)(t-4m^2)]^{1/2}}\right). \quad \text{(C41)}$$

This is valid only for $t>4m^2$, but the extension to the region $4\mu^2<t<4m^2$ is straightforward:

$$\bar\rho(t)=\frac{1}{4}\left(\frac{t-4\mu^2}{t}\right)^{1/2}\frac{1}{t-4m^2}\left\{\frac{t-2\mu^2}{[(t-4\mu^2)(4m^2-t)]^{1/2}}\times\arctan\frac{t-2\mu^2}{[(t-4\mu^2)(4m^2-t)]^{1/2}}-1\right\}, \quad t<4m^2. \quad \text{(C42)}$$

The function $\bar\rho(t)$ is continuous at $t=4m^2$; its value at that point is

$$\bar\rho(4m^2)=\frac{1}{48m^2}\frac{(1-\mu^2/m^2)^{3/2}}{(1-\frac{1}{2}\mu^2/m^2)^2}. \quad \text{(C43)}$$

Let us notice another useful relation:

$$G_1+2(6m^2-s-2t)G_2+(s-4m^2)G_5=8m^2(G_2+G_4), \quad \text{(C44)}$$

where $G_i\equiv G_i(s,t)$. This corresponds to the Feynman graph of Fig. 29. We now give the expressions for the partial-wave amplitudes:

$$f_{12}{}^{J,1}=-\alpha^2\frac{2ms^{1/2}}{\pi(s-4m^2)}\gamma\frac{[J(J+1)]^{1/2}}{2J+1}\times(H_{12}{}^{J+1}-H_{12}{}^{J-1}), \quad \text{(C45)}$$

$$f_{12}{}^{J,0}=9f_{12}{}^{J,1}, \quad \text{with} \quad \gamma=\left(\frac{s-4m^2}{s}\right)^{1/2},$$

where

$$H_{12}{}^J(s)=\int_{4\mu^2}^{\infty}\bar\rho(t')Q_J\left(1+\frac{2t'}{s-4m^2}\right)dt', \quad \text{(C46)}$$

$$f_{11}{}^{J,1}=\frac{\gamma\alpha^2}{\pi}\left\{\frac{1}{2J+1}\frac{4m^2}{s-4m^2}\times[(J+1)H_{12}{}^{J+1}+JH_{12}{}^{J-1}]+X^J\right\}, \quad \text{(C47)}$$

$$f_{11}{}^{J,0}=9f_{11}{}^{J,1},$$

$$f_0{}^{J,1}=\frac{\gamma\alpha^2}{\pi}\left(\frac{4m^2}{s-4m^2}H_{12}{}^J+X^J\right), \quad \text{(C48)}$$

$$f_0{}^{J,0}=9f_0{}^{J,1},$$

$$f_{22}{}^{J,1}=\frac{\gamma\alpha^2}{\pi}\left\{\frac{1}{2J+1}\frac{4m^2}{s-4m^2}[(J+1)H_{12}{}^{J-1}+JH_{12}{}^{J+1}]+\frac{J+1}{2J+1}Y^{J-1}+\frac{J}{2J+1}Y^{J+1}+Y^J\right\}, \quad \text{(C49)}$$

$$f_{22}{}^{J,0}=9f_{22}{}^{J,1},$$

$$f_1{}^{J,1}=\frac{\gamma\alpha^2}{\pi}\left(\frac{4m^2}{s-4m^2}H_{12}{}^J+\frac{J+1}{2J+1}Y^{J-1}+\frac{J}{2J+1}Y^{J+1}+Y^J\right), \quad \text{(C50)}$$

$$f_1{}^{J,0}=9f_1{}^{J,1},$$

and

$$H_{12}{}^J=\int_{4\mu^2}^{\infty}\bar{\rho}(t')Q_J\left(1+\frac{2t'}{s-4m^2}\right)dt', \quad \text{(C51)}$$

$$X^J=\int_{4\mu^2}^{\infty}\mathrm{Im}_tX(s,t')Q_J\left(1+\frac{2t'}{s-4m^2}\right)dt', \quad \text{(C52)}$$

$$Y^J=\int_{4\mu^2}^{\infty}\mathrm{Im}_tY(s,t')Q_J\left(1+\frac{2t'}{s-4m^2}\right)dt', \quad \text{(C53)}$$

$$\mathrm{Im}_tX=\frac{1}{s-4m^2}\left[4m^2\bar{\rho}(t)-\frac{1}{4}\left(\frac{t-4\mu^2}{t}\right)^{1/2}-\frac{\mu^4}{t^{1/2}\Delta}\bar{R}(s,t)\right], \quad \text{(C54)}$$

$$\mathrm{Im}_tY=\frac{1}{(4m^2-s-t)^2}\left\{[t^2-2m^2(4m^2-s+t)]\bar{\rho}(t)+\frac{4m^2-s+t}{8}\left(\frac{t-4\mu^2}{t}\right)^{1/2}+\frac{t(4m^2-s)(t-4\mu^2)+2\mu^4(4m^2-s+t)}{4t^{1/2}\Delta}\bar{R}(s,t)\right\}, \quad \text{(C55)}$$

where $\bar{R}(s,t)=-\psi(s,t)$ is defined in (C37) and $\Delta$ in (C35).

We notice that these formulas are valid only for $J\neq 0$; for $J=0$ (i.e., for the ${}^1S_0$ and ${}^3P_0$ waves), we cannot use the Froissart-Gribov formula; in fact the integral (C52) is divergent for $J=0$, as is quite obvious. For these waves the calculation proceeds as follows: After some trivial manipulations, one has for the contribution of the direct graph

$$f_1=\tfrac{1}{4}\alpha^2\left[(s-4m^2)\frac{(2G_2-G_5)}{\alpha^2}+4m^2\frac{(G_2+G_4)}{\alpha^2}\right], \quad \text{(C56)}$$

$$f_2=\tfrac{1}{4}\alpha^2\left[(s-4m^2)\frac{(2G_2-G_5)}{\alpha^2}+4m^2\frac{(G_2+G_4)}{\alpha^2}z\right], \quad \text{(C57)}$$

so that taking into account the interchange of final nucleons:

$$f_0{}^{0,1}=\gamma\int_{-1}^{1}f_1dz=\frac{\gamma\alpha^2}{\pi}\left(T_0+\frac{4m^2}{s-4m^2}H_{12}{}^0\right), \quad \text{(C58)}$$

$$f_{11}{}^{0,1}=\gamma\int^{1}f_2dz=\frac{\gamma\alpha^2}{\pi_{-1}}\left(T_0+\frac{4m^2}{s-4m^2}H_{12}{}^1\right), \quad \text{(C59)}$$

where

$$T_0=\tfrac{1}{4}\pi(s-4m^2)\int_{-1}^{1}Xdz. \quad \text{(C60)}$$

The quantity $X$ is defined by

$$X=\frac{t}{\pi}\int_{4\mu^2}^{\infty}\frac{\mathrm{Im}_tX}{t'(t'-t)}dt'+(X)_{t=0}, \quad \text{(C61)}$$

where

$$(X)_{t=0}=(2/\alpha^2)(G_4)_{t=0}. \quad \text{(C62)}$$

One has, obviously,

$$(G_4)_{t=0}=\frac{1}{\pi}\int_{4\mu^2}^{\infty}\frac{\mathrm{Im}_tG_4(s,t')}{t'}dt'. \quad \text{(C63)}$$

Finally, after some additional calculations, the following formula for $T_0$ is obtained:

$$T_0=\tfrac{1}{2}(s-4m^2)\int_{4\mu^2}^{\infty}\frac{\mathrm{Im}_tX(s,t')}{t'}\times\left[Q_1\left(1+\frac{2t'}{s-4m^2}\right)-Q_0\left(1+\frac{2t'}{s-4m^2}\right)\right]dt'+(s-4m^2)\int_{4\mu^2}^{\infty}\frac{\bar{\rho}(t')-\bar{r}(s,t')}{t'}dt', \quad \text{(C64)}$$

where

$$\bar{r}(s,t')=\frac{1}{8u(t)^{1/2}}\left[2\bar{R}\left(\frac{t}{u}-\frac{2\mu^4}{(s-4m^2)(t-4\mu^2)-4\mu^4}\right)+\frac{8(t)^{1/2}}{u}\bar{\rho}(t)[(t-4\mu^2)(s-4m^2)-u(s-2m^2)]+(t-4\mu^2)^{1/2}\left(2\frac{s-4m^2}{u}-\frac{1}{2}\frac{(s-4m^2)(t-4\mu^2)-2\mu^4}{\mu^4+m^2(t-4\mu^2)}\right)-2\frac{s-2m^2}{t-4m^2}(t-4\mu^2)^{1/2}\left(1-\frac{(t-2\mu^2)^2}{4\mu^4+4m^2(t-4\mu^2)}\right)\right] \quad \text{(C65)}$$

and $\mathrm{Im}_tX$ is defined in (C54).

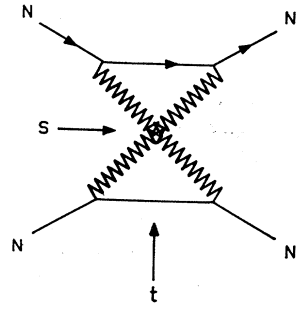


FIG. 30. Crossed-box diagram in the $N$-$N$ elastic amplitude.

### 6. Crossed-Box Diagram

The diagram to be computed now is represented in Fig. 30. We find that the contribution of this graph to the $G_i^T$ amplitudes can always be expressed in terms of the three functions $B$, $B_1$, and $B_2$ defined by Eqs. (C24). The explicit expression is

$$G_1^0=(3\alpha^2/32\pi)\{3s[B_1(u,t)-B_1(t,u)]+4[tB_1(u,t)-uB_1(t,u)]+(4m^2-s)[B_2(u,t)-B_2(t,u)]+8[B(u,t)-B(t,u)]\}, \quad \text{(C66)}$$

$$G_1^1=-(\alpha^2/32\pi)\{15s[B_1(u,t)+B_1(t,u)]+20[tB_1(u,t)+uB_1(t,u)]+5(4m^2-s)[B_2(u,t)+B_2(t,u)]+40[B(u,t)+B(t,u)]\}, \quad \text{(C67)}$$

$$G_2^0=-(3\alpha^2/32\pi)\{-s[B_1(u,t)+B_1(t,u)]+(4m^2-s)[B_2(u,t)+B_2(t,u)]\}, \quad \text{(C68)}$$

$$G_2^1=-(\alpha^4/32\pi)\{5s[B_1(u,t)-B_1(t,u)]-5(4m^2-s)[B_2(u,t)-B_2(t,u)]\}, \quad \text{(C69)}$$

$$G_3^0=-(3\alpha^2/32\pi)\{s[B_1(u,t)-B_1(t,u)]+(4m^2-s)[B_2(u,t)-B_2(t,u)]+4[B(u,t)-B(t,u)]\}, \quad \text{(C70)}$$

$$G_3^1=-(\alpha^2/32\pi)\{-5s[B_1(u,t)+B_1(t,u)]-5(4m^2-s)[B_2(u,t)+B_2(t,u)]-20[B(u,t)+B(t,u)]\}, \quad \text{(C71)}$$

$$G_4^0=-(3\alpha^2/32\pi)\{-s[B_1(u,t)+B_1(t,u)]-(4m^2-s)[B_2(t,u)+B_2(u,t)]-4[B(u,t)+B(t,u)]\}, \quad \text{(C72)}$$

$$G_4^1=-(\alpha^2/32\pi)\{5s[B_1(u,t)-B_1(t,u)]+5(4m^2-s)[B_2(u,t)-B_2(t,u)]+20[B(u,t)-B(t,u)]\}, \quad \text{(C73)}$$

$$G_5^0=-(3\alpha^2/32\pi)\{s[B_1(u,t)-B_1(t,u)]+3(4m^2-s)[B_2(u,t)-B_2(t,u)]-4[tB_2(u,t)-uB_2(t,u)]+8[B(u,t)-B(t,u)]\}, \quad \text{(C74)}$$

$$G_5^1=-(\alpha^2/32\pi)\{-5s[B_1(u,t)+B_1(t,u)]-15(4m^2-s)[B_2(u,t)+B_2(t,u)]+20[tB_2(u,t)+uB_2(t,u)-40[B(u,t)+B(t,u)]\}. \quad \text{(C75)}$$

If we now define

$$B^J(s)=\frac{8}{\pi(s-4m^2)}\left[\int_{4\mu^2}^{\infty}\mathrm{Im}_t B(4m^2-s-t',t')Q_J\left(1+\frac{2t'}{s-4m^2}\right)dt' +(-1)^J\int_{4m^2}^{\infty}\mathrm{Im}_s B(s',4m^2-s-s')Q_J\left(1+\frac{2s'}{s'-4m^2}\right)ds'\right], \quad \text{(C76)}$$

$$B_i^J(s)=\frac{8}{\pi(s-4m^2)}\left[\int_{4\mu^2}^{\infty}\mathrm{Im}_t B_i(4m^2-s-t',t')Q_J\left(1+\frac{2t'}{s-4m^2}\right)dt' +(-1)^J\int_{4m^2}^{\infty}\mathrm{Im}_s B_i(s',4m^2-s-s')Q_J\left(1+\frac{2s'}{s'-4m^2}\right)ds'\right], \quad i=1,2 \quad \text{(C77)}$$

the partial-wave amplitudes can be immediately obtained, and are expressed by the following formulas:

$$f_0^{J,1}=-\frac{5}{8}\gamma\frac{\alpha^2}{32\pi}\left[s(s+4m^2)B_1^J-(4m^2-s)^2B_2^J-8(2m^2-s)B^J -s(4m^2-s)\left(\frac{J+1}{2J+1}B_1^{J+1}+\frac{J}{2J+1}B_1^{J-1}\right)-(4m^2-s)^2\left(\frac{J+1}{2J+1}B_2^{J+1}+\frac{J}{2J+1}B_2^{J-1}\right)\right], \quad \text{(C78)}$$

$$f_0^{J,0}=-\tfrac{3}{5}f_0^{J,1},$$

$$f_{11}^{J,0}=\frac{3}{8}\gamma\frac{\alpha^2}{32\pi}\left[16m^2\frac{J}{2J+1}B^{J-1}+s(s+4m^2)\frac{J}{2J+1}B_1^{J-1}-\frac{J}{2J+1}(4m^2-s)^2B_2^{J-1}+8(s-4m^2)B^J+s(s-4m^2)B_1^J -(4m^2-s)^2B_2^J+61m^2\frac{J+1}{2J+1}B^{J+1}+s(s+4m^2)\frac{J+1}{2J+1}B_1^{J+1}-(4m^2-s)^2\frac{J+1}{2J+1}B_2^{J+1}\right], \quad \text{(C79)}$$

$$f_{11}^{J,1}=-(5/3)f_{11}^{J,0},$$

$$f_{12}^{J,0}=-\tfrac{3}{2}\gamma\frac{\alpha^2}{32\pi}ms^{1/2}\frac{[J(J+1)]^{1/2}}{2J+1}[s(B_1^{J+1}-B_1^{J-1})+2(B^{J+1}-B^{J-1})], \quad \text{(C80)}$$

$$f_{12}{}^{J,1}=-(5/3)f_{12}{}^{J,0},$$

$$f_{22}{}^{J,0}=+\tfrac{3}{8}\gamma\frac{\alpha^2}{32\pi}\Big[4s\frac{J+1}{2J+1}B^{J-1}+s(s+4m^2)\frac{J+1}{2J+1}B_1{}^{J-1}-(4m^2-s)^2\frac{J+1}{2J+1}B_2{}^{J-1}+4(s-4m^2)B^J+s(s-4m^2)B_1{}^J$$
$$-(4m^2-s)^2B_2{}^J+4s\frac{J}{2J+1}B^{J+1}+s(s+4m^2)\frac{J}{2J+1}B_1{}^{J+1}-(4m^2-s)^2\frac{J}{2J+1}B_2{}^{J+1}\Big], \quad \text{(C81)}$$

$$f_{22}{}^{J,1}=-(5/3)f_{22}{}^{J,0},$$

$$f_1{}^{J,0}=\tfrac{3}{8}\gamma\frac{\alpha^2}{32\pi}\Big[s(s+4m^2)B_1{}^J-(4m^2-s)^2B_2{}^J+4sB^J-s(4m^2-s)\Big(\frac{J}{2J+1}B_1{}^{J+1}+\frac{J+1}{2J+1}B_1{}^{J-1}\Big)$$
$$-(4m^2-s)^2\Big(\frac{J}{2J+1}B_2{}^{J+1}+\frac{J+1}{2J+1}B_2{}^{J-1}\Big)+4(s-4m^2)\Big(\frac{J}{2J+1}B^{J+1}+\frac{J+1}{2J+1}B^{J-1}\Big)\Big], \quad \text{(C82)}$$

$$f_1{}^{J,1}=-(5/3)f_1{}^{J,0},$$

where

$$\mathrm{Im}_sB(s,t)=\frac{\pi}{(st)^{1/2}}\frac{1}{s-4m^2+t}\Big[\Big(\frac{t}{s-4m^2}\Big)^{1/2}(s-4m^2+2\mu^2)\ln\Big(\frac{s-4m^2+\mu^2}{\mu^2}\Big)-[(s-4m^2)(t-4\mu^2)-4\mu^4]^{1/2}$$
$$\times\ln\Big(\frac{[t(s-4m^2)]^{1/2}+[(s-4m^2)(t-4\mu^2)-4\mu^4]^{1/2}}{[t(s-4m^2)]^{1/2}-[(s-4m^2)(t-4\mu^2)-4\mu^4]^{1/2}}\Big)+i\pi[(s-4m^2)(t-4\mu^2)-4\mu^4]^{1/2}\Big], \quad \text{(C83)}$$

when

$$s>4m^2,\quad t>4\mu^2\Big(1+\frac{\mu^2}{s-4m^2}\Big);$$

$$\mathrm{Im}_sB(s,t)=\frac{\pi}{(st)^{1/2}}\frac{1}{s-4m^2+t}\Big[(s-4m^2+2\mu^2)\Big(\frac{t}{s-4m^2}\Big)^{1/2}\ln\Big(\frac{s-4m^2+\mu^2}{\mu^2}\Big)$$
$$-2[(s-4m^2)(4\mu^2-t)+4\mu^4]^{1/2}\arctan\frac{[t(s-4m^2)]^{1/2}}{[(s-4m^2)(4\mu^2-t)+4\mu^4]^{1/2}}\Big], \quad \text{(C84)}$$

when

$$s>4m^2,\quad 0<t<4\mu^2\Big(1+\frac{\mu^2}{s-4m^2}\Big);$$

$$\mathrm{Im}_sB(s,t)=\frac{\pi}{(-st)^{1/2}}\frac{1}{s-4m^2+t}\Big[\Big(\frac{-t}{s-4m^2}\Big)^{1/2}(s-4m^2+2\mu^2)\ln\Big(\frac{s-4m^2+\mu^2}{\mu^2}\Big)$$
$$-[(s-4m^2)(4\mu^2-t)+4\mu^4]^{1/2}\ln\frac{[-t(s-4m^2)]^{1/2}+[(s-4m^2)(4\mu^2-t)+4\mu^4]^{1/2}}{-[-t(s-4m^2)]^{1/2}+[(s-4m^2)(4\mu^2-t)+4\mu^4]^{1/2}}\Big], \quad \text{(C85)}$$

when $s>4m^2$, $t<0$.

The absorptive parts in $s$ of $B_1$ and $B_2$ are obtained by the usual relations:

$$\mathrm{Im}_sB_1(s,t)=\frac{\partial}{\partial m^2}\mathrm{Im}_sB(s,t;m^2,\mu^2),$$
$$\mathrm{Im}_sB_2(s,t)=\mathrm{Im}_sB_1(s,t)+4\frac{\partial}{\partial s}\mathrm{Im}_sB(s,t;m^2,\mu^2). \quad \text{(C86)}$$

It can easily be seen that the integrals in Eqs. (C76) and (C77) are convergent for all values of $J$, so that for this graph there is no particular problem in computing the $^1S_0$ and $^3P_0$ partial-wave contributions.

## APPENDIX D

### 1. One-Pion Contribution to Partial-Wave Nucleon-Nucleon Amplitudes

We use the formulas of Appendix C. We recall that $\alpha$ is the renormalized coupling constant $\alpha=g^2/4\pi$.

For isospin 1, the contribution to the singlet amplitude is

$$f_0{}^{J,1}(s)=\frac{\alpha\mu^2}{s-4m^2}\Big(\frac{s-4m^2}{s}\Big)^{1/2}Q_J\Big(1+\frac{2\mu^2}{s-4m^2}\Big)$$
$$-\frac{\alpha}{2}\Big(\frac{s-4m^2}{s}\Big)^{1/2}\delta_{J,0}. \quad \text{(D1)}$$

Only even values of $J$ are physical; we notice that all waves Reggeize except the $J=0$ ($^1S_0$ state). When we say that the wave Reggeizes (or does not Reggeize) it is only for the one-pion contribution; no conclusion can be drawn for the total amplitude. However, in perturbation theory, it is found that when the one-pion contribution (Born term) Reggeizes, the remaining part of the amplitude does the same and vice-versa.

The contribution to the triplet amplitude is

$$\begin{aligned}
&f_{11}{}^{J,1}(s)=-f_0{}^{J,1}(s),\\
&f_{12}{}^{J,1}(s)=0,\\
&f_{22}{}^{J,1}(s)=-\tfrac{1}{2}\alpha\left(\frac{s-4m^2}{s}\right)^{1/2}\left[Q_J\left(1+\frac{2\mu^2}{s-4m^2}\right)\right.\\
&\qquad-\frac{J+1}{2J+1}Q_{J-1}\left(1+\frac{2\mu^2}{s-4m^2}\right)\\
&\qquad\left.-\frac{J}{2J+1}Q_{J+1}\left(1+\frac{2\mu^2}{s-4m^2}\right)\right].
\end{aligned}\tag{D2}$$

Here again, only even values of $J$ are physical, and all waves Reggeize, except the $J=0$ ($^3P_0$ state). We notice that

$$(^1S_0)_{(1\text{ pion})}=-(^3P_0)_{(1\text{ pion})}.\tag{D3}$$

Finally, the contribution to the uncoupled triplet is

$$f_1{}^{J,1}(s)=-f_{22}{}^{J,1}(s).\tag{D4}$$

Here only odd values of $J$ are physical; all waves Reggeize.

For isospin zero, we use the relation

$$f^{J,0}(s)=-3f^{J,1}(s).\tag{D5}$$

Of course, we must now interchange odd and even for the physical values of $J$, and all waves Reggeize because the value $J=0$ for the uncoupled triplet is forbidden.

It is useful to reexpress the triplet amplitude in a new basis, connected to the previous one by the formulas

$$\begin{aligned}
f_{J-1,J-1}&=\frac{1}{2J+1}\{Jf_{11}{}^J+(J+1)f_{22}{}^J\\
&\qquad+2[J(J+1)]^{1/2}f_{12}{}^J\},\\
f_{J-1,J+1}&=\frac{1}{2J+1}\{[J(J+1)]^{1/2}\\
&\qquad\times[f_{22}{}^J-f_{11}{}^J]-f_{12}{}^J\},\\
f_{J+1,J+1}&=\frac{1}{2J+1}\{(J+1)f_{11}{}^J+Jf_{22}{}^J\\
&\qquad-2[J(J+1)]^{1/2}f_{12}{}^J\}.
\end{aligned}\tag{D6}$$

The reason for introducing the unitary transformation (D6) is that these new amplitudes must have the following threshold behavior:

$$\left.\begin{aligned}
&f_{J-1,J-1}\sim p^{2J-1}\\
&f_{J-1,J+1}\sim p^{2J+1}\\
&f_{J+1,J+1}\sim p^{2J+3}
\end{aligned}\right\}\text{when } p=\text{c.m. momentum}\to 0.\tag{D7}$$

The one-pion contribution to these new waves, for $I=1$, yields

$$\begin{aligned}
f_{J-1,J-1}{}^{I=1}(s)&=\frac{-\alpha}{2(2J+1)}\left(\frac{s-4m^2}{s}\right)^{1/2}\left[Q_J\left(1+\frac{2\mu^2}{s-4m^2}\right)-Q_{J-1}\left(1+\frac{2\mu^2}{s-4m^2}\right)\right],\\
f_{J-1,J+1}{}^{I=1}(s)&=\frac{-\alpha}{2(2J+1)}\left(\frac{s-4m^2}{s}\right)^{1/2}[J(J+1)]^{1/2}\\
&\qquad\times\left[2Q_J\left(1+\frac{2\mu^2}{s-4m^2}\right)-Q_{J-1}\left(1+\frac{2\mu^2}{s-4m^2}\right)-Q_{J+1}\left(1+\frac{2\mu^2}{s-4m^2}\right)\right],\\
f_{J+1,J+1}{}^{I=1}(s)&=\frac{-\alpha}{2(2J+1)}\left(\frac{s-4m^2}{s}\right)^{1/2}\left[Q_{J+1}\left(1+\frac{2\mu^2}{s-4m^2}\right)-Q_J\left(1+\frac{2\mu^2}{s-4m^2}\right)\right].
\end{aligned}\tag{D8}$$

It then follows from formulas (D8) that

$$\begin{aligned}
&f_{J-1,J-1}{}^{(1\text{ pion})}\sim p^{2J+1},\\
&f_{J-1,J+1}{}^{(1\text{ pion})}\sim p^{2J+1},\\
&f_{J+1,J+1}{}^{(1\text{ pion})}\sim p^{2J+3}.
\end{aligned}\tag{D9}$$

To summarize, we see that the one-pion contribution will give rise to a correct threshold behavior in all waves except

(a) the $f_{J-1,J-1}$ waves,
(b) the $^1S_0$ wave.

We notice that the $^3S_1$ deuteron $s$ wave belongs to set (a).

## 2. Threshold Behavior of Partial-Wave Amplitudes in Framework of Padé Approximations

### A. Scalar Case

In this case the coefficients $S_n(p)$ of the $S$ matrix expansion

$$S(g,p)=1+S_1(p)g+S_2(p)g^2 +\cdots+Sn(p)g^n+\cdots, \quad \text{(D10)}$$

are ordinary functions of $p$. If we suppose first that $S_1\equiv 0$, the $[1,1]$ does not exist but the other $[N,N]$ approximants exist and have a correct threshold behavior. This can be easily seen by looking at the explicit form of the approximants given in Ref. 7. Now, if $S_1(p)$ vanishes at threshold faster than the other terms $S_i(p)$, only the $[1,1]$ approximant has a pathological behavior. This is what happens in the $N$-$N$ problem.

### B. Matrix Case

We restrict ourself to the case in which the coefficients of the series $S_i(p)$ are $2\times 2$ matrices. The generalization to $r\times r$ matrices is obvious.

Near threshold we have, in angular momentum $J$,

$$S_n{}^J(p)=p^{2J-1}I(p^2)A_n{}^J(p)I(p^2), \quad \text{(D11)}$$

with

$$I(p^2)=\begin{bmatrix}1 & 0\\ 0 & p^2\end{bmatrix}. \quad \text{(D12)}$$

In the limit $p\to 0$, the matrix $A^J$ is, in general, a matrix with constant and nonzero elements. On the other hand, since $I(p^2)$ does not depend on $g$, it is equivalent to take the Padé approximant of $S^J$ or of $A^J$.

In the $N$-$N$ case the limit of the matrix $A_{(1)}{}^J(p)$ is of the form

$$\begin{bmatrix}0 & \alpha\\ \alpha & \beta\end{bmatrix}.$$

The first element is zero, but this does not imply that $A_1{}^J$ is a singular matrix, and in this respect the matrix case clearly differs from the scalar case. Moreover, if we multiply $A_{(1)}{}^J$ by some other constant matrices, as we have to do in order to calculate Padé approximants, the resulting matrix has no reason (in general) to have a vanishing element. The result is of the form

$$[N,N]=1+p^{2J-1}I(p^2)B_{[N,N]}I(p^2), \quad \text{(D13)}$$

where the elements of $B_{[N,N]}$ are quite generally nonzero. Hence, the behavior is no longer pathological. This is true for any value of $N$, and in particular for the $[1,1]$ Padé approximation.

## 3. More Complete Study of $J=1$, $T=0$ Wave

### A. Scattering Region

The $S$ matrix is a $2\times 2$ matrix defined by

$$S^{J=1,T=0}=I+iF^{J=1,T=0}, \quad \text{(D14)}$$

where $I$ is the unit matrix and $F$ is the symmetric matrix:

$$F^{J=1,T=0}=\begin{pmatrix}f_S & f_{SD}\\ f_{SD} & f_D\end{pmatrix}. \quad \text{(D15)}$$

Elastic unitarity reads

$$2\,\mathrm{Im}F=FF^*=F^*F. \quad \text{(D16)}$$

Time-reversal invariance implies that $S$ is real in the region of analyticity:

$$4m^2-\mu^2<s<4m^2. \quad \text{(D17)}$$

There are two standard ways for parametrizing (D14). Either one diagonalizes $S$,

$$S=U^{-1}e^{2i\Delta}U, \quad \text{(D18)}$$

with

$$U=\begin{bmatrix}\cos\epsilon_1 & \sin\epsilon_1\\ -\sin\epsilon_1 & \cos\epsilon_1\end{bmatrix} \quad \text{(D19)}$$

and

$$\Delta=\begin{bmatrix}\delta_0 & 0\\ 0 & \delta_2\end{bmatrix}; \quad \text{(D20)}$$

one then gets the set of equations

$$\begin{aligned}1+if_S&=\cos^2\epsilon_1\,e^{2i\delta_0}+\sin^2\epsilon_1\,e^{2i\delta_2},\\ 1+if_D&=\cos^2\epsilon_1\,e^{2i\delta_2}+\sin^2\epsilon_1\,e^{2i\delta_0},\\ if_{SD}&=\tfrac{1}{2}\sin 2\epsilon_1\,(e^{2i\delta_0}-e^{2i\delta_2}).\end{aligned} \quad \text{(D21)}$$

Notice that for $s-4m^2\to 0$ it can be shown that[31]

$$\epsilon_1\approx Qk^2 \quad (s=4m^2+4k^2), \quad \text{(D22)}$$

where $Q$ is the electric quadrupolar moment of the deuteron. Or one defines another parametrization of $S$ as

$$S=\exp(i\bar{\delta})\exp(2i\bar{\epsilon})\exp(i\bar{\delta}), \quad \text{(D23)}$$

where $\bar{\delta}$ is a diagonal matrix, and $\bar{\epsilon}$ is an antidiagonal matrix:

$$\bar{\delta}=\begin{pmatrix}\bar{\delta}_0 & 0\\ 0 & \bar{\delta}_2\end{pmatrix} \quad \text{and} \quad \bar{\epsilon}=\begin{pmatrix}0 & \bar{\epsilon}_1\\ \bar{\epsilon}_1 & 0\end{pmatrix}. \quad \text{(D24)}$$

In that case one has

$$\begin{aligned}1+if_S&=\cos 2\bar{\epsilon}_1\exp(2i\bar{\delta}_0),\\ 1+if_D&=\cos 2\bar{\epsilon}_1\exp(2i\bar{\delta}_2),\\ if_{SD}&=i\sin 2\bar{\epsilon}_1\exp[i(\bar{\delta}_0+\bar{\delta}_1)].\end{aligned} \quad \text{(D25)}$$

This set of phase shifts is known under the name of "bar-phase shifts."

[31] L. C. Biedenharn and J. M. Blatt, Phys. Rev. **93**, 1387 (1954).

In order to get from Eq. (D21) to Eq. (D25) we need the formulas

$$\begin{aligned} &\delta_0+\delta_2=\bar{\delta}_0+\bar{\delta}_2, \\ &\sin(\delta_0-\delta_2)=(\sin 2\bar{\epsilon}_1)/\sin 2\epsilon_1, \\ &\sin(\bar{\delta}_0-\bar{\delta}_2)=(\tan 2\bar{\epsilon}_1)/\tan 2\epsilon_1. \end{aligned} \tag{D26}$$

In particular, we deduce the threshold behavior of $\bar{\epsilon}_1$:

$$\bar{\epsilon}_1 \cong a_t \epsilon_1 k \propto a_t Q k^3. \tag{D27}$$

(We have made our phase shift start from zero, whereas the usual convention is that the $s$-wave phase shift starts at $+\pi$, owing to the presence of the deuteron pole in the amplitude.) Experimentally, $a_t$ is positive and $Q$ is also positive, so that $\bar{\epsilon}_1$ must start with a positive value. In our model, we obtain $a_t$ and $Q$ with the correct sign as was shown above; it then follows that our sign of $\bar{\epsilon}_1$ is also automatically correct.

### *B. Deuteron Parameters*

We shall use here nonrelativistic language in order to clarify the relation between physical quantities and the deuteron pole residues.

It is well known that one can go from the scattering waves $u_0$ and $w_0$, which for $r \to \infty$ behave as

$$\begin{aligned} &u_0 \xrightarrow[r\to\infty]{} \frac{\cos\epsilon_1}{\sin\delta_0}\sin(kr+\delta_0)\equiv \bar{u}_0, \\ &w_0 \xrightarrow[r\to\infty]{} \frac{\sin\epsilon_1}{\sin\delta_0}\sin(kr-\pi+\delta_0)\equiv \bar{w}_0, \end{aligned} \tag{D28}$$

to the deuteron wave functions, $u_d$ and $w_d$ which for $r \to \infty$ behave as

$$\begin{aligned} &u_d \xrightarrow[r\to\infty]{} \cos\epsilon_d\, e^{-(mB)^{1/2}r}\equiv \bar{u}_d, \\ &w_d \xrightarrow[r\to\infty]{} \sin\epsilon_d\, e^{-(mB)^{1/2}r}\equiv \bar{w}_d, \end{aligned} \tag{D29}$$

by an analytical continuation in $k$. In fact, by putting $k=+i(mB)^{1/2}$ in (D28), we get (D29) provided we take into account the condition

$$\cot\delta_0\big|_{k=+i(mB)^{1/2}} = +i \quad \text{(bound-state condition)}. \tag{D30}$$

One then finds

$$\epsilon_1\big|_{k=i(mB)^{1/2}} = -\epsilon_d. \tag{D31}$$

On the other hand, we get from Eq. (D21)

$$\tan 2\epsilon_1 = 2f_{SD}/(f_S-f_D), \tag{D32}$$

which at the deuteron pole becomes

$$\tan 2\epsilon_d = -2R_{SD}/(R_S-R_D) \tag{D33}$$

and gives the solution

$$\rho=\tan\epsilon_d=-R_{SD}/R_S. \tag{D34}$$

In the same way, one obtains the "effective range" of the deuteron:

$$\begin{aligned} \rho(-B_1-B) &\equiv 2\int_0^\infty (\bar{u}_d{}^2+\bar{w}_d{}^2-u_d{}^2-w_d{}^2)dr \\ &= \frac{1}{(mB)^{1/2}} - 2\int_0^\infty (u_d{}^2+w_d{}^2)dr, \end{aligned} \tag{D35}$$

which is found to be, after a straightforward calculation,

$$\rho(-B_1-B)=\frac{1}{(mB)^{1/2}}+i\frac{16(mB)^{1/2}}{R_S+R_D}. \tag{D36}$$

In particular, we see that $R_S$ and $R_D$ must be purely imaginary numbers, *with a negative imaginary part.*